A tale of two mechanisms: The p53 modulator COTI-2 is a Zn metallochaperone

İrem Şimşek[1†], Farsheed Shahbazi-Raz[1,2†*], Michael J. Krause[1‡], Azam Mohammadzadeh[1‡], Maryam Kosar[1,3], Peihan Xu[1], Samra Khan[1], Olena Tykhoniuk[1], Ashley DaDalt[1,4], Deya'a Almasri[1], Lara K. Watanabe[1,5], Kaitlyn Breault[1], John J. Hayward[1,6], Fraser S. Pick[1], Richard L. Ho[7], Jeremy M. Rawson[1], John F. Trant[1,2,6,8*]

[1] Department of Chemistry and Biochemistry, University of Windsor, Windsor, ON, N9B 3P4, Canada

[2] Binary Star Research Services, LaSalle ON, N9J 3X8, Canada

[3] Current Address: IRIC, Université de Montréal, Montréal, QC, H3T 1J4, Canada

[4] Current Address: Department of Natural Sciences, University of Michigan Dearborn, Dearborn, MI 48128, USA

[5] Current Address: Department of Chemistry, University of Guelph, Guelph, ON, N1G 2W1, Canada

[6] Department of Biomedical Sciences, University of Windsor, Windsor, ON, N9B 3P4, Canada

[7] Amaro Therapeutics, New York, NY, 10036, USA

[8] WE-Spark Research Institute, Windsor, ON, N9B 3P4, Canada

[†] These authors contributed equally to the work and may rearrange the order of their names for any professional purpose, names are listed strictly in alphabetical order and this does not imply greater contribution by one or the other.

[‡] These authors contributed equally to the work and may rearrange the order of their names for any professional purpose, names are listed strictly in alphabetical order and this does not imply greater contribution by one or the other.

* Corresponding authors' email: *farsheed@uwindsor.ca; j.trant@uwindsor.ca*

Abstract: (275 words)

Mutations in, or misregulation of, *Tp53* are found in approximately 50% of all cancers. p53 functions by ensuring that cells with irretrievably damaged DNA undergo apoptosis. When p53 is non-functional in cells that may also be undergoing uncontrolled cell growth (due to other mutations), cancer readily emerges. Consequently, restoring the function of misregulated and mutated *Tp53* is an incredibly important goal in therapeutic oncology. *Tp53* mutations often induce conformational changes that inhibit the protein's ability to engage its DNA response element. Small molecule refolding guides could theoretically restore the proper shape and activity, but this is a far more challenging design problem than the typical paradigm of designing enzymatic inhibitors. Consequently, it is unsurprising that there are no approved p53-targeting drugs. **COTI-2**, a thiosemicarbazone with orphan-drug status for ovarian cancer, has proven an effective cytotoxic agent against various cancer cell lines *in vitro*, exhibited efficacy *in vivo*, and has demonstrated a good safety profile in Phase 1b human clinical trials. The proposed mechanism—direct engagement and refolding of mutant p53—has been derived from a combination of cell-based assays and transcriptomics data. We propose that this is an unlikely mechanism of action, and that instead **COTI-2** is acting as a selective, well-tolerated, zinc chaperone to replace zinc ions lost to p53 mutants' deficient zinc-binding. We discuss that **COTI-2** likely also works through other mechanisms but demonstrate that zinc-binding is necessary for the exceptional bioactivity. The promising therapeutic potential of this molecule and additional evidence for its zinc chaperone activity is discussed. This would make it the first well-tolerated zinc chaperone with pharmacological implications not only for cancer but for other zinc deficiency-related diseases.

Keywords: restoration-of-function, metallochaperone, apoptosis, personalized medicine, chemotherapy

Introduction

The tumor suppressor gene *Tp53* plays a pivotal role in regulating cell fate, acting as a shield against tumorigenesis by directing irretrievably damaged cells toward apoptosis.[1-3] The protein functions by tetramerizing (from dimeric subunits in solution) at specific DNA sequences in the nucleus, initiating protein expression.[4-5] One of the expressed proteins (p21) then arrests the cell cycle at the G1/S transition, stimulating DNA repair; should this fail, other p53-promoted pathways initiate apoptosis.[4] The ability of p53 to destroy damaged cells is so critical that over 50% of all cancers have a *Tp53* mutation: without this mutation, the cells (regardless of the nature of other mutations) would have been slated for apoptosis and would not have proceeded to form a tumor.[6-9] Some studies go further, proposing that specific *Tp53* mutations cause the protein to gain additional functionality to drive tumorigenesis in addition to losing its regulatory activity.[7, 10] Hotspot mutants of the protein have consequently been of significant interest as a target for the generation of drugs that can either restore its function,[1, 6, 11] or inhibit the pathways that lead to its degradation;[12-15] these drugs, should they prove successful, could potentially combat a significant number of cancers. It is, however, far more complicated to ensure proper protein folding than it is to inhibit a typical enzyme,[16] and this approach has not yet found clinical success.

p53 is a multi-domain protein comprising a series of protein-binding motifs in the N and C-terminal regions, including the tetramerization domain that allows for the formation of a stable complex around a central DNA-sequence binding domain.[17] This domain includes a zinc-binding site. The Zn^{2+} ion is non-catalytic—its role is simply to ensure the proper tertiary folds are formed to provide the sequence specificity.[18] However, the loss of zinc unfolds this protein providing a different control mechanism for p53 regulation—zinc concentration. Unfortunately, this reliance on the cationic cofactor also makes the protein sensitive to mutations that can disrupt zinc binding.[19-20] The most prominent *Tp53* hotspot mutations include R175H and R273H, residues found in the DNA-binding domain near the zinc-binding site.[7, 21-24] The former is a structural mutant, causing conformational distortions that compromise zinc binding without interfering with the DNA binding capacity.[18-19, 25] The latter is at the DNA-interface and inhibits binding to DNA.[7, 26-27] Both mutants disrupt p53's ability to modulate regulatory pathways.[7, 26-28]

Among various potential therapeutic strategies, small molecule reactivation of mutant p53 is potentially feasible.[1, 8, 11] Various reagents restore inactive mutant p53 to wild-type activity, but the precise mode of action remains unknown. Crystallography, while crucial for protein structure

determination, doesn't fully capture protein behavior, especially if the key interactions are weak and highly dynamic and the protein complex is large and effectively impossible to crystallize in its native state.[29] Experimental structural biology can be complemented by computational modeling to provide insight into the mechanism.[29] Combining these methods has led to the identification of the Y220C reactivation pocket (**Figure S1A**),[30-31] the L1/S3 binding pocket (**Figure S1B**),[32] and the S6-S7 pocket of the V143A mutant (**Figure S1C**).[33] These sites have been targeted with multiple small molecules with varying success such as **CP-31398**[34], **STIMA-1**[35], **PRIMA-1**[36], and **GK02723** & **CD04879** (**Figure 1**).[37-38]

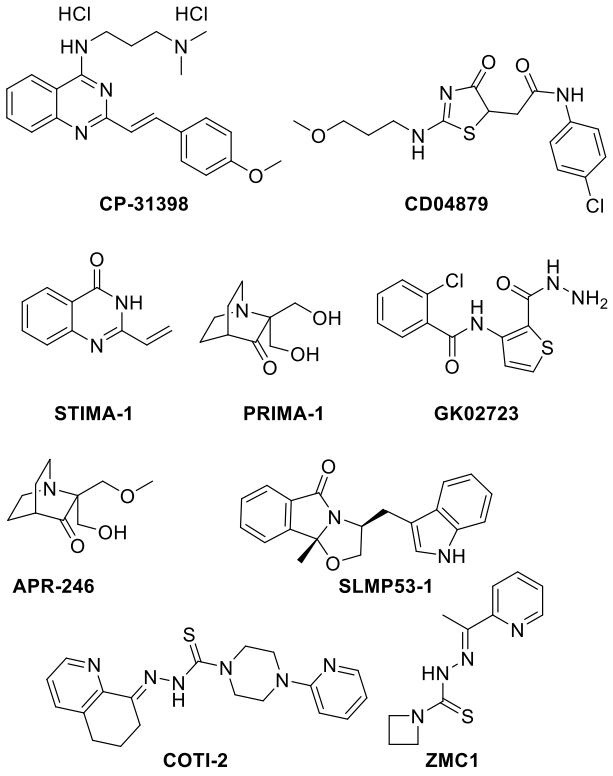

Figure 1. Structures of several p53-targeting drugs discussed in this report.

Despite this preclinical progress, p53 is still generally considered "undruggable;"[1, 39] however, two compounds with proposed reactivation activity have entered clinical trials: **APR-246** and **COTI-2**.[40] **APR-246**, a covalent trap-containing molecule, is methylated **PRIMA-1**, this modification enhancing membrane permeability.[17, 41-42] **APR-246** has been proposed to refold specific mutant p53s, reactivating them while showing tolerable toxicity.[17, 41-44] These inferences have been built on biochemical and cell biology results; however, recent data has shown that it is active even in p53-deficient cells,[45-46] and that activity is in fact independent of p53 mutation state,

and that the covalent trap drug seems to act through a non-specific inhibition of many different proteins.[47] The second drug, **COTI-2** has also been proposed as a p53-mutant refolding chaperone, but there is a dearth of data demonstrating target engagement; furthermore, although there is suggestive data, the precise mutants susceptible to treatment remain unconfirmed. However, the preliminary Phase 1b clinical data has been promising showing that it could help patients.[48-50]

COTI-2 is a third-generation thiosemicarbazone introduced by Cotinga,[49] and developed using the CHEMSAS computational tool.[51] It has potent cytotoxic (reported single-digit nM in standard MTT assays) activity against a wide range of human cancer cells.[51-52] **COTI-2** has also been shown to be effective *in vivo*, and is the first thiosemicarbazone to enter Phase 1 clinical trials.[1, 49, 51] Currently, Phase 1b trials have been successfully completed for both gynecological and head and neck squamous cell carcinoma (HNSCC) showing safety,[48-50] and the drug has orphan status from the FDA for ovarian cancer.[53] **COTI-2** works synergistically when combined with cisplatin or radiotherapy, precisely the result expected for a p53-restoration-of-function molecule.[48-50] The capacity of **COTI-2** to restore function to p53 mutants in HNSCC tumor cells was demonstrated using chromatin immunoprecipitation experiments.[49, 54] Additionally, **COTI-2** augments the expression levels of the p53 down-regulator MDM2. However, a proteomic analysis of **COTI-2** exposure in some cell lines reveals changes in expression levels of targets independent of the p53 pathway, primarily downstream products of the mTOR pathway, suggesting that there is also a p53-independent mechanism of action.[49]

The anti-proliferative activity of **COTI-2** is more potent on cell lines with mutant p53 than on cells with wild-type p53, supporting some form of mutant activity restoration. Exposure to **COTI-2** was shown, using conformation-specific antibodies, to induce a conformational change of mutant p53 in SKBR3 ($Tp53_{R175H}$) cells into a conformation more in-line with the wildtype.[55] Along with these results, biophysical surface plasmon resonance (SPR) data provides target engagement evidence that **COTI-2** can bind to both full-length and DNA-binding domain-only mutant p53 forms, although admittedly only with a weak K_D at the μM level, three orders of magnitude below the cytotoxic dose.[55] The mode of action consequently remains unclear.[17, 43]

The structure of **COTI-2** might provide some clues. As a thiosemicarbazone proximate to nitrogen heterocycles, one would expect it to have strong chelating capacity for metals, particularly iron, copper, and zinc.[48, 51] There is biochemical evidence that **COTI-2** can be inactivated by copper.[56] However, of these metals, zinc is particularly interesting as it is crucial for proper p53

protein folding: the zinc ion is coordinated by C^{176} and H^{179} from the L2 loop and by C^{238} and C^{242} from the L3 loop. Loss of the zinc ion causes these loops to unfold, inactivating p53. Mutations in these coordinating amino acids eliminate p53 function, while mutations in nearby residues reduce zinc affinity, decreasing protein stability, by misaligning these amino acids.[18-19] Among structural mutations, $Tp53_{R175H}$ is the most frequent; severely affecting p53 stability and function.[10, 23, 57] Zinc binding by **COTI-2** has been dismissed based on some preliminary biochemical studies,[49] but this conclusion seems highly unlikely based on the fundamental co-ordination chemistry of this functional group.

ZMC1 is an established zinc metallochaperone that restores the activity of zinc-binding mutants of *Tp53*.[58-59] **ZMC1** acts as a zinc ionophore, transporting zinc ions into the cells, and then buffering zinc to reactivate p53 zinc-binding mutants.[19, 58-59] **ZMC1** binds Zn^{2+} ~100-fold stronger than serum albumin and thus can readily strip the metal from the latter source.[20] The zinc affinity of **ZMC1** has been measured to be 81 nM by stoichiometric titration;[60] metallochaperones for p53 should have Zn^{2+} K_d values on the order of 10-50 nM to ensure facile transfer to the protein, but still bind well to the metal. This is lower than zinc affinity at the native p53 site ($K_{d1} \approx 2\ nM$) but far higher than affinity at mutated sites when in the induced zinc-free conformation where the histidines drop away from one another making the required tetravalency impossible ($K_{d2} \geq 1\ \mu M$).[61] This suggests that if it could localize to the nucleus, **ZMC1** could unload zinc to favour a native-like fold in the p53 (which would then have an affinity value for DNA closer to the wild-type). An equilibrium dialysis experiment supported the contention that **ZMC1**'s activity did not involve a direct interaction with the p53-DNA binding domain (**DBD**). This evidence combines to suggest that **ZMC1** activates mutant p53 by restoring normal zinc loading, raising intracellular (and potentially intranuclear) zinc concentrations, and improving zinc binding to DBD, rather than *via* traditional drug-protein binding and modifying protein function/conformation.[20, 62] Das and Mukhopadhyay's study employing various computational techniques implies that **ZMC1** may not directly interact with the p53-DBD_{R175H} mutant but could bind to the $p53_{R175H}$ mutant at the L2-L3 region, forming specific interactions with neighboring residues R^{174} and P^{190}.[63] This would not have been observed with a truncated DBD mutant, but might explain co-localization.

Although there appears to have been no previous joint consideration of the drug **COTI-2** and the probe molecule **ZMC1**, the shared co-ordinating motif encouraged us to investigate whether **COTI-2** likewise acts through a zinc-dependent mechanism and perhaps acts as a

metallochaperone instead of a structural binding refolder of p53. After all, $p53_{R175H}$, reduces but does not abrogate zinc binding, if a drug could restore the presence of zinc, $p53_{R175H}$ could recover the conformation, and likewise the function, of the wildtype. The lack of any previous convincing target engagement data for **COTI-2** makes this a worthwhile mechanism for investigation, and we employed a variety of computational and experimental methods to demonstrate that zinc mediation is a likely mechanism of action.

Materials and Methods

For additional details beyond those described here, please see the supplementary information.

Synthetic Chemistry

For the general experimental protocol, including instruments used for analysis, purification and source of reagents, and the synthesis of **COTI-2**, **Zn(COTI-2)$_2$** and **Ru(COTI-2)$_2$** please see the supplementary information (**Scheme S1**). The synthesis was modified from the published patents.[64-65]

Cell Culture and Biological Assays

Human cell lines were purchased from the American Type Culture Collection (ATCC, Manassas, VA, USA) including HCT116 (colon cancer) cells, SKBR3 (breast adenocarcinoma) cells, KLE (endometrial cancer) cells, Capan-2 (pancreatic cancer) cells, and H1299 (lung) cells. HCT116 cells were cultured in DMEM, KLE cells in DMEM/F12 media, and Capan-2 and SKBR3 cells in McCoy's 5 A medium (Thermo Fisher Scientific). All culture media were supplemented with 10% Fetal Bovine Serum (Millipore-Sigma, F1051) and 1% Penicillin-Streptomycin (10,000 U/mL). Cell cultures were maintained at 37 °C in a 5% CO_2 environment. For additional information on cell culture and the CETSA and cycloheximide chase assays, please see Sections 1.3 and 1.4 of the Supporting Information.

Statistical Analysis

All the graphs, calculations, and statistical analyses were conducted using GraphPad Prism 8.0.2. (263) for Windows (GraphPad Software, Inc, Boston MA). A two-way ANOVA, Dunnett's method, was used to compare the means of each treatment group with the control group, allowing

for multiple comparisons. Each data point was presented as the mean ± standard deviation, with statistical significance indicated by P values of 0.05 or less.

Isothermal Titration Calorimetry

Calorimetric experiments were performed employing a low-volume reaction cell Affinity calorimeter from TA instruments. Zn^{2+} and $Ru^{2+/3+}$ solutions were prepared at 0.1 mM concentration in distilled water and 1% DMSO. **COTI-2** was diluted to a final concentration of 0.1 mM in distilled water and 1% DMSO. All measurements were carried out at 25 ºC. Each titration comprised fifty 1.5 μL injections. The cell was loaded with the metal ion solutions at 0.01 mM concentration, and the syringe with the **COTI-2** solution. All injections were performed using an initial injection of 1.5 μL followed by 49 injections of 1.5 μL of 0.1 mM **COTI-2**. The data were analyzed with the TA NanoAnalyze software package, excluding the first data point in the fit calculations. Thermodynamic parameters were calculated using the equation $\Delta G = \Delta H - T\Delta S = -RT(\ln K)$, where ΔG, ΔH, and ΔS represent changes in free energy, enthalpy, and entropy of binding, respectively, R is the ideal gas constant, and K is the equilibrium constant for the process.

Computational details

For a detailed discussion of the computational methods, please see section 1.5 of the Supporting Information.

Result and discussion

COTI-2 is cytotoxic against human cancer cell lines.

As a first step, we sought to confirm that our in-house synthetic batch of **COTI-2** (>99.5% purity) acted the same as the material used in previous reports (99.0-99.9 % purity); we have found discrepancies with reagents used in other studies conducted by our group where we identified that activity previously reported by others likely arose from impurities in the sample.[66] We found it difficult to find published characterization data, and it is provided here as a courtesy to readers.[i] **COTI-2** sensitive cell lines were treated with the drug for 72 hours (**Figure 2**). As per reports from the Duffy group,[55] **COTI-2**'s cytotoxicity appeared largely independent of *Tp53* mutation status, and it was active at low nanomolar concentrations. The IC_{50} values are generally consistent, if a

[i] . For research quantities of COTI-2, please contact the corresponding author; these are available on a collaborative basis to the community while supplies are present.

little bit higher, than previous reports;[51, 55] however, this deviation is well within expected lab-to-lab variability. The synthetic batch prepared in our lab appears to have the same activity as that previously generated, and the previous activity is not due to the presence of a synthetic impurity.

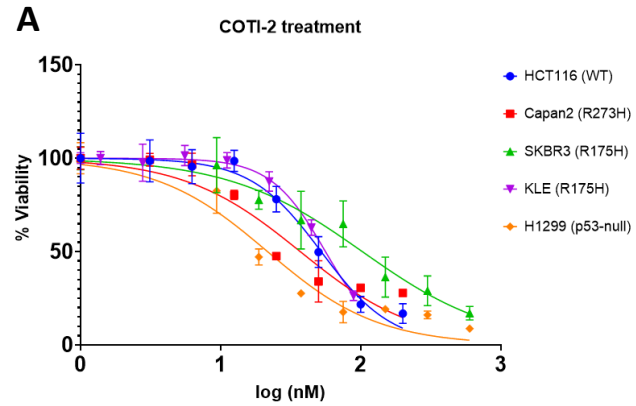

Cell Line$_{p53\ status}$	HCT116$_{WT}$	Capan-2$_{R273H}$	SKBR3$_{R175H}$	KLE$_{R175H}$	1299$_{p53\text{-}null}$
IC_{50} (nM)	52.2	37.0	102.7	56.0	21.6

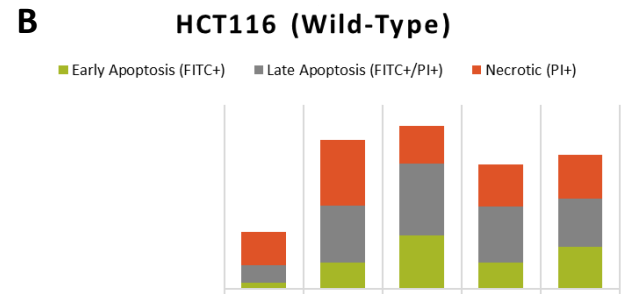

	0μM	0.5μM	1μM	5μM	10μM
Necrotic (PI+)	9.0%	17.9%	10.3%	11.5%	12.0%
Late Apoptosis (FITC+/PI+)	4.9%	15.6%	19.6%	15.3%	13.1%
Early Apoptosis (FITC+)	1.6%	7.1%	14.5%	7.1%	11.4%

Figure 2. COTI-2 is cytotoxic and works through an apoptotic mechanism. **A) COTI-2** induced cytotoxicity on different human cancer cell lines with 72 hours exposure to the drug. The IC_{50} values were interpolated from the curves fit to the data using GraphPad Prism 8. The IC_{50} values in the table are in nM. The graph shown represents data from at least three different technical replicates each of three different biological replicates, involving different subcultures of cells collected on different weeks. Error bars represent the standard deviation of these nine measurements. **B)** Flow Cytometry Analysis of Annexin V-FITC/PI (PE) Experiment, arising from three biological replicates. Representative data plots are provided in the SI as **Figure S3.**

Based on the IC_{50} value findings, **COTI-2** demonstrated effectiveness in killing cells at low nanomolar concentrations. The cell-killing effect of **COTI-2** was further assessed using a clonogenic assay, a common method to evaluate the efficacy of cancer treatments in reducing tumor cell survival. Following treatment with **COTI-2**, cells were allowed to grow in the absence of **COTI-2** to assess the level of cell death induced by **COTI-2** compared to the control (**Figure**

S2). **COTI-2** decreased the viability of the KLE cell line by over 50% at a concentration of 40 nM compared to the vehicle control, completely in line with the MTT assay. The reduction in cell viability was further supported by the observed decrease in cell colony formation following **COTI-2** treatment at various concentrations.

We then confirmed the apoptotic potential of **COTI-2**; if acting through a p53-related pathway, this would be the expected mechanism of cell death (**Figure 2B**, **Figure S3**). Using the Annexin-V FITC/PI flow cytometry assay,[68] most cells remained viable at the 24 hour mark (as they did in the MTT assay, this is expected) with increased progression to apoptosis at 500 nM compared to the untreated control. Further increases in drug concentration did not meaningfully shift the ratios of the cell populations, supporting an apoptosis-directed mechanism of toxicity. This evidence is all in line with the analyses of others proposing a p53-related pathway; however, this does not necessarily imply direct target engagement at the molecular level.

COTI-2 does not appear to directly engage p53

It has been generally supposed that **COTI-2**'s activity arises from its direct interaction with mutant p53 to induce a return to wild-type folding and functionality; however, it is unclear how that occurs.[17, 49, 55] One of the challenges in studying a drug against p53 using any in-cell assay is that one is almost always inevitably measuring downstream events rather than direct target engagement. Cell-free assays are challenging as the protein has no enzymatic activity, and the drug target may be the tetrameric-p53 (**Tet-p53**) complex with DNA rather than a single domain or dimer of p53 in solution,[4] complicating biophysical analysis. Indirect surrogate measurements of differential drug effects on p53 mutants are confounded by all the other differences between cell lines other than their *Tp53* status. Consequently, we treated H1299 cells, a viable *Tp53* double knock-out line, with **COTI-2** as a negative control. We intended to use this cell line as a stable vector to explore **COTI-2**'s efficacy against different *Tp53* mutants, aiming to transfect the cells with a series of *Tp53*-mutant-bearing plasmids. The unexpected high efficacy of **COTI-2** against this *Tp53*-null cell line redirected our work. If **COTI-2** functions primarily by engaging p53 or Tet-p53, then one would expect a *Tp53*-null cell-line to be resistant to effects. This is clearly not the case: **COTI-2** was most toxic to this cell line. The mechanism of **COTI-2** cannot be even primarily through a direct engagement with p53.

A comprehensive examination of the literature, both academic, patent, and internal Cotinga data does not provide any experiment that conclusively demonstrates target engagement. The assumption that the effect stems from direct interaction seems to emerge from biochemical, transcriptomic, phenotypic, and metabolomic assays that show an effect consistent with the restoration of p53 function. All extant evidence measures downstream effects rather than p53 engagement itself and does imply that mutant p53 activity is restored in the presence of **COTI-2** in a dose dependent manner. However, this hypothesis is not supported by the data.

There is a single SPR experiment,[55] but this is less convincing than it could be; it shows that both full-length $p53_{R273C}$ and DBD-only p53 (DBD_{R175H}) interact with **COTI-2** with K_d values on the order of single digit μM with very short residency times.[55] However, the drug is effective at doses as low as single digit nM. This suggests that activity is unrelated to p53 binding, and that the binding observed is weak if present at all. However, as this was done with a monomer (it being difficult to envision preparing a stable tetramer with DNA in sufficient purity and with sufficient stability to analyze by SPR), this data is difficult to interpret as it is unclear if engagement with monomeric p53 is biologically meaningful. Consequently, we sought alternative methods to demonstrate evidence of target engagement.

Thermal shift assays fail to show evidence of target engagement

The cellular engagement thermal shift assay (CETSA) confirms target engagement as small-molecule binding almost universally increases the stability of a protein target, raising the thermal stability of the protein.[69-70] The effect should be apparent as both a function of drug concentration at a constant temperature, or a function of temperature at a constant drug concentration. The effect should also be apparent across multiple cell lines if the candidate drug can co-localize with the target protein and avoid cellular metabolism over the timeframe of the study. CETSA assays can also be conducted on cell lysates should metabolism prove a problem. CETSA is certainly not appropriate for all proteins—especially low abundant multidomain proteins like Tet-p53,[71] but this objection is not sustained as CETSA *has* been successfully, and repeatedly, used under the same conditions we applied for Tet-p53–probe molecules that do bind the protein directly.[72-73] We examined HCT-116, SKBR3, Capan2, and KLE cancer cells with their different p53 mutants under many different CETSA conditions (**Figures S4** & **S5**).

In total, we ran over 100 independent CETSA experiments under a variety of different parameters (cell lines, temperature gradients, incubation times, drug concentrations, cell

incubation conditions, lysis conditions, denaturation conditions, *etc.*); in none of the studies did we see any clear evidence of target engagement, and thermal stability was never reproducibly different from the DMSO vehicle. This same null-result was obtained whether we conducted CETSA on the whole cell, or on the lysate.[73-74]

The cycloheximide chase assay fails to show evidence of target engagement.

Cycloheximide blocks protein translation, preventing a replenishment of protein. This allows one to measure protein half-life; or to determine if half-life is extended through binding to small molecules.[75-77] The cycloheximide assay has been used to demonstrate target engagement with Tet-p53 in the past.[76, 78] As with the CETSA, we see no increase in stability in the presence of **COTI-2**, even at concentrations over a 1000-fold higher than the effective concentration (**Figure S5c** & **S6**).

Although these experimental assays failed to show potent interactions between Tet-p53 and **COTI-2**—expected to be observed if the drug works by binding to induce a refolding—they are consistent with weak transient engagement should the drug work through an alternative mechanism. To explore where **COTI-2** might interact, we turned to *in silico* investigations.

In silico *analyses do not support the existence of a high affinity direct interaction between* ***COTI-2*** *and Tet-p53*

Mutations in *Tp53* likely only matter if they affect the assembly or conformation of the tetramer-DNA complex.[79-80] Analysis is complicated as we do not know where on Tet-p53 **COTI-2** might bind; for our study we assumed that the drug binds somewhere on the structurally well-resolved DNA-binding or tetramerization domains rather than on the disordered linkers or protein termini. This assumption is reasonable based on the mutants affected, but is also technically necessary, as accurate sampling and screening of small molecule binding to these conformational dynamic unstructured domains is not currently feasible.

To find likely sites for binding to the properly folded Tet-p53$_{WT}$ bound to the requisite zinc cofactors and DNA sequence (**WT-Zn**), we employed the Schrödinger SiteMap tool (Schrödinger Release 2021-3, New York, NY, USA) on the structure of the full length Tet-p53 structure developed by Amaro,[81] based on the crystal structure (PDB: *3TS8*) reported by Halazonetis;[82] this led to the identification of two feasible binding sites, both positioned proximate to the DNA: **Site-1** and **Site-2** (**Figure 3**).

Site-1 sits between p53 monomers A and B in the DBD directly adjacent to their zinc atoms. **Site-2** is in an analogous position between monomers C and D (**Figure 3**). These sites overlap with the site, previously identified by Gomes and colleagues, as the target for p53-binder **SLMP53-1**,[83] which acts by compensating for the loss of a DNA-contact in $p53_{K280X}$ mutants to restore DNA-binding.[72]

Binding pockets can be crudely categorized as "druggable", "difficult", and "undruggable."[84] Undruggable sites are small and highly hydrophilic, difficult sites are a suitable size but largely hydrophilic, while druggable sites are appropriately sized and more hydrophobic. SiteMap ranks sites taking these features into account to generate a Dscore. Binding pockets with Dscores lower than 0.83 are likely "undruggable", pockets with Dscores above 0.98 are "druggable", and those with Dscores in between are "difficult".[85] For **WT-Zn,** the Dscore of **Site-1** is 0.83 and that of **Site-2** is 0.82. When the zinc ions are removed (**WT-noZn**), the Dscore of **Site-1** rises to 0.98. Therefore, **Site-1** could be a potential binding site for binding **COTI-2**.

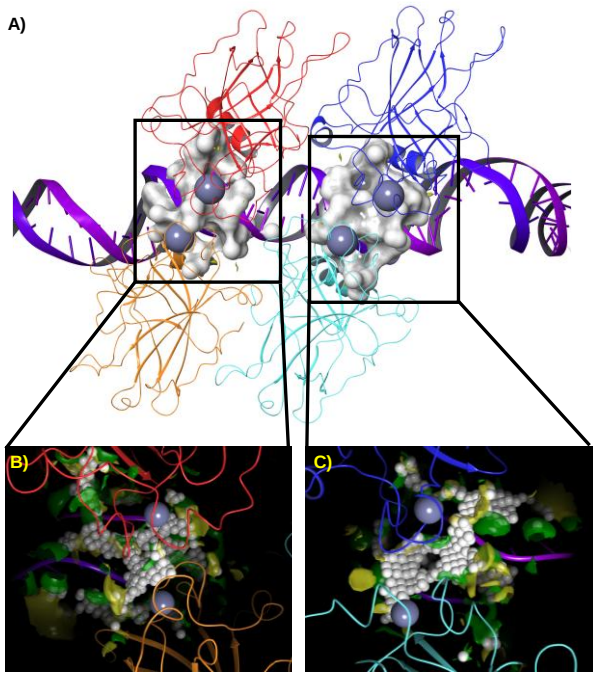

Figure 3. Potential binding sites of Tet-p53 explored and characterized using SiteMap; **A)** Relative positions of **Site-1** (left) and **Site-2** (right) in the Tet-p53–DNA pentaplex; **B)** expansion of **Site-1**; **C)** expansion of **Site-2**. Hydrophilic regions are divided into hydrogen bond donor (green) and acceptor (yellow) regions. The white spheres denote SiteMap points that are placed into a 4 Å grid

and used as a binding site for docking **COTI-2**. The images are colour coded: p53 units A (orange), B (red), C (cyan) and D (blue) and DNA (purple).

We used the Schrödinger suite to perform induced-fit molecular docking of **COTI-2** at **Site-1**. In all cases of our preliminary analysis, the binding at **Site-1** was far stronger than the binding at **Site-2** so the latter was not considered in detail. The poses were ranked by the Glide docking score (**Table S1**), and the lowest energy pose was feasible by inspection (**Figure 4**). The proposed binding mode for **COTI-2** at **Site-1** for **WT-Zn**, **WT-noZn** and mutants **R175H-Zn**, **R175H-noZn**, **R273H-Zn** and **R273H-noZn** are presented in **Figure 4**. **COTI-2** interacts with both monomers A and B and the DNA in all structures. The calculated log *P* value for **COTI-2** is 2.9, indicating moderate lipophilicity.[56] The bulky hydrocarbon components of the molecule are available to interact with M^{243} in both units and L^{137} and C^{242} of monomer A in **WT-Zn** (**Figures 4A and S7A**). The docking scores for the binding of **COTI-2** to **WT-Zn** and **WT-noZn** are −5.2 and −8.43 kcal/mol, respectively (**Table S1**). This difference arises because removing the zinc atom allows for a relaxation of loop-3 (L3)—containing zinc-binding C^{242}—by over 1 Å, which allows for M^{243} to swing into position to make an H-bond with the sulfur atom of **COTI-2** (**Figure 4B**). Likewise, this scissors open the gap between L2 and L3 (previously glued together by zinc) exposing the DNA for a better interaction with **COTI-2** (**Figures 4C** & **S7B**). A similar pattern, and affinity, is observed with zinc-binding mutant **R175H** (−7.25 and −8.49 kcal/mol, respectively for **R175H-Zn** and **R175H-noZn**; **Figures 4D, 4E, 4F, S7C** & **S7D**). **COTI-2** has only poor affinity for either form of the DNA-binding mutant **R273H** (**Figures S7E** & **S7F**). Regardless, even the best docking scores here are moderate, and single digit nM affinity would not be expected from any of these binding modes.

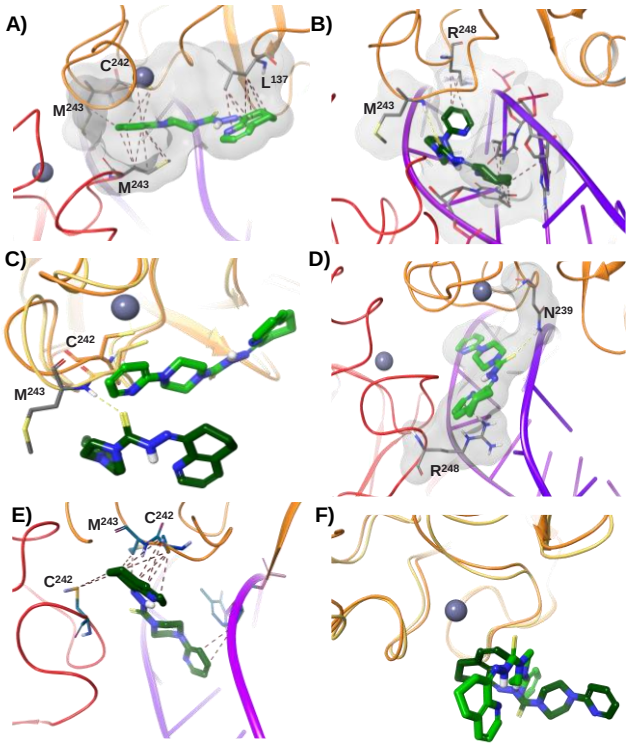

Figure 4. Visualization of the predicted binding mode of **COTI-2** at **Site-1** with **A) WT-Zn**; **B) WT-noZn**; **C)** superimposition of the previous two panels—WT with (pale green and orange) and without Zn (dark green and yellow); **D) R175H-Zn**; **E) R175H-noZn** structures; **F)** superimposition of the previous two panels—**R175H** with (pale green, orange) and without (dark green and yellow) Zn. Colors: **COTI-2** (pale green in structures with Zn, and dark green in structures without Zn), H-bond (yellow dash), hydrophobic bonds (brown dash), π-cation (dark-green dashed), p53 units A (orange/yellow), B (red) and DNA (purple).

There is no evidence that COTI-2 directly engages p53 at the high affinity suggested by the potent activity.

Both the CETSA and cycloheximide chase assays are designed to specifically identify protein-ligand engagement. Neither one suggested that binding occurs. Like others working with Tet-p53, we recognize that direct biophysical tools are challenging to employ,[86-88] but both CETSA and cycloheximide have been used routinely.[72, 89-91] We could find no examples of these two simple assays being employed for **COTI-2**; it is possible that the results did not support the hypothesis that **COTI-2** binds p53, the major consensus in the literature, and so were not reported in the relevant studies. The computational study also failed to suggest a strong binding mode to the

protein. It is important to note that these studies do not mean that **COTI-2** does not bind p53/Tet-p53, but rather that the affinity is not sufficient to explain the nM efficacy of the agent; these negative results, coupled with the potent cytotoxicity against a p53-null cell line, strongly suggest that it is unlikely that the observed activity is through direct binding to p53. The basis of activity most likely lies elsewhere even if it generally still correlates strongly with p53 mutant status.

Synthesis and characterization of the Zn(COTI-2)$_2$ complex

If direct binding and the induction of refolding is not indicated, what other mechanisms could be operable?[17, 49, 55] Zinc homeostasis is essential for p53 activity and regulation.[18-20, 25, 62] As discussed above, the zinc metallochaperone **ZMC1**, which works by modulating zinc levels in cells, shares the pyridinyl-thiosemicarbazone functional group with **COTI-2**. Although dismissed in a previous study, we firmly believe that **COTI-2** must bind zinc, and so we investigated **COTI-2**'s affinity for the ion.

ZMC1 forms complexes with Zn^{2+} in a 2:1 ratio,[60] confirmed by the X-ray crystal structure of the **Zn(ZMC1)$_2$** complex where the two deprotonated **ZMC1** molecules bind to Zn^{2+}, forming a neutral octahedral complex at the thiosemicarbazone, typical of the functional group.[92] This trivalent co-ordination is provided by the thiocarbonyl sulphur anion, the thiocarbonyl β-nitrogen, and pyridinyl nitrogen.[61] The K_d values of **ZMC1** with zinc was measured to be ~3×10^{-8} M by stoichiometric titration.[60] Substituting the thiocarbonyl group with a carbonyl group reduced zinc affinity by about 100-fold (K_d=1.1×10^{-6} M).[60]

Based on structural similarity (**Figure 4** & **Video. S1**), one would expect similar values for zinc-binding with **COTI-2**. These have never, to the best of our knowledge, been measured. We accessed **Zn(COTI-2)$_2$** by treating two equivalents of **COTI-2** with one equivalent of $ZnCl_2$ in refluxing ethanol in the presence of excess triethylamine to induce tautomerization (Error! Reference source not found.). An X-ray crystal structure of the resultant complex was obtained from small crystals generated from recrystallization of a toluene solution (**Figure 5C**, **Figure S8** & **Table S2**).

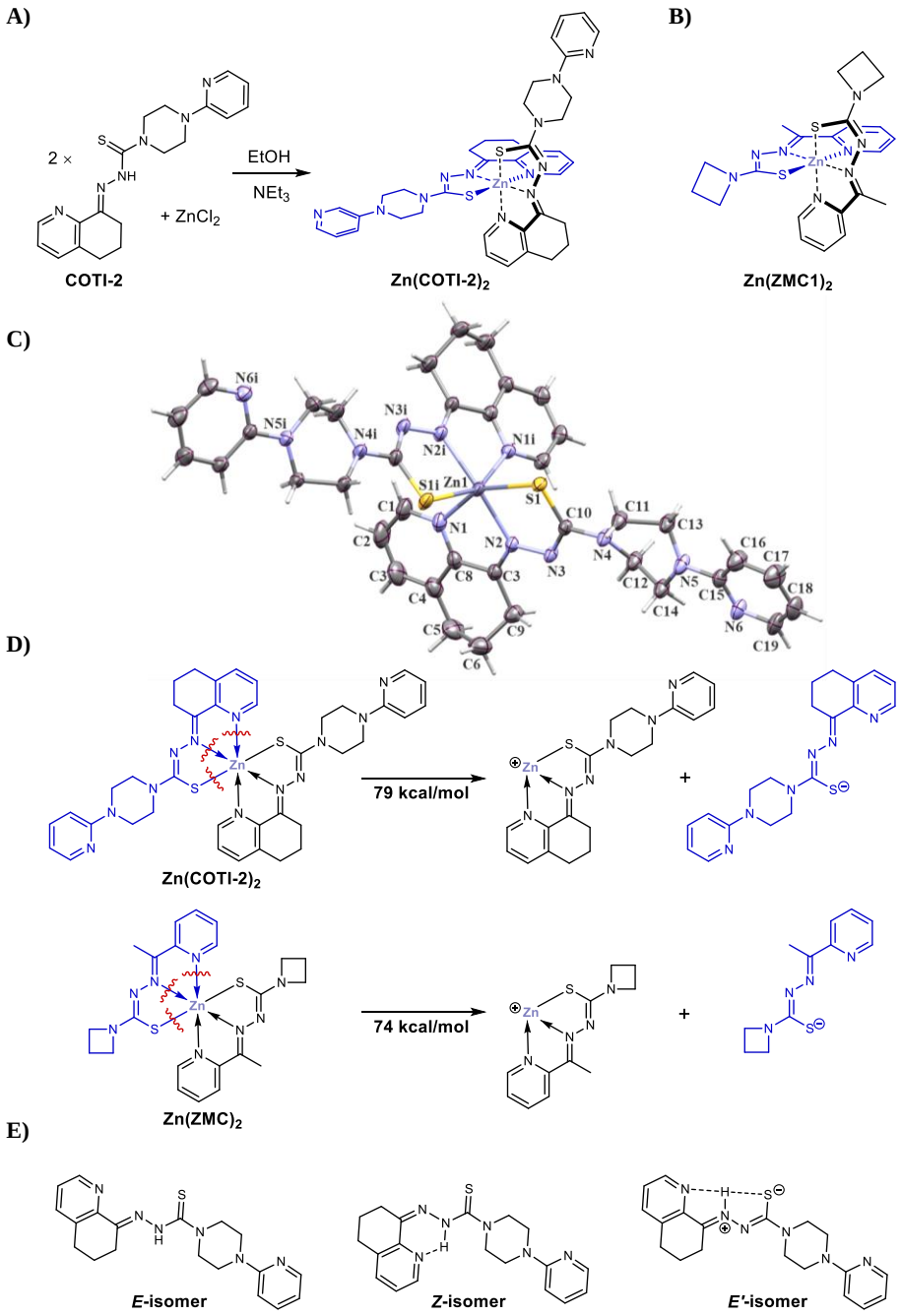

Figure 5. (A) Synthesis of *mer*-**Zn(COTI-2)$_2$**, (B) Structure of *mer*-**Zn(ZMC1)$_2$** and (C) The labeled diagram of the X-ray crystal structure of **Zn(COTI-2)$_2$** (thermal ellipsoids are at the 50% probability level); the two **COTI-2** molecules sit perpendicular to each other around the zinc atom. Note that in the literature, the **Zn(ZMC1)$_2$** complex was drawn as being in the *fac*- configuration although the accompanying crystal structure has it in the same *mer*- form as determined for *mer*-**Zn(COTI-2)$_2$**.[60] (D) Dissociation of **Zn(COTI-2)$_2$** and **Zn(ZMC1)$_2$** complexes into the ligand and metal species, and (E) different possible isomers of **COTI-2**.

The asymmetric unit comprises one crystallographically unique molecule of *mer*-**Zn(COTI-2)$_2$** in which the Zn(II) displays octahedral coordination geometry with four coordinated N atoms in the equatorial plane and two axial S atoms from the two tridentate **COTI-2** ligands. The four Zn-N bond lengths can be split into two Zn-pyridinyl N bond lengths—2.205(2) and 2.273(2) Å—and two shorter Zn-imine bond lengths—2.158(2) and 2.133(2) Å—potentially reflecting stronger bonding of the imine-N to the Zn(II) site (**Table S3**). The Zn–S distances (2.4305(6) – 2.4685(6) Å) are a little longer, as expected for the larger S atom. These values for **Zn(COTI-2)$_2$**, are similar to those in **Zn(ZMC1)$_2$**: 2.13, 2.21 and 2.45 Å.[61] The C–S bond lengths (1.723(2) – 1.730(2) Å) are closer to typical C–S single bonds (1.74 Å) than C=S bonds (1.65 Å), indicative of substantial single bond character, which supports tautomerization of **COTI-2**, and anionic thiolate character. The same effect is seen in **Zn(ZMC1)$_2$**.

The crystallographically determined structure may not necessarily reflect the solution-phase or isolated nature of these molecules: intermolecular interactions, by definition, will distort the structure from what would be found in the physiological environment. To explore these differences, we employed density functional theory (DFT).

Ligand-metal dissociation energies from DFT calculations and the design of alternative complexes

The optimised geometry of **Zn(COTI-2)$_2$** in the gas phase remains very similar to that in the crystal structure (**Table S3**). What is also clear is that it is highly similar to **Zn(ZMC1)$_2$**, including the expected ligand dissociation energies (LDE, 73.65 kcal/mol for **ZMC1**, 78.95 for **COTI-2**). The latter are a bit tougher to calculate as we are not looking at complex disassembly, nor are we looking at the cleavage of a single bond, but rather we need three bonds simultaneously to release to remove a ligand from zinc. This is an unlikely event and leads to very strong bonds between the ligand and the zinc (**Figure 5D**). Blanden and colleagues experimentally attempted to measure **ZMC1** binding with Zn^{2+} using a competition assay with a fluorescent zinc chelator, estimating a K_d of 3×10^{-8} M. We chose to measure the affinity of **COTI-2** for zinc directly using isothermal titration calorimetry (**Figure S9A**); this provided a similar estimate of affinity, with a measured K_d of 6.58×10^{-8} M. The accuracy of ITC measurements are generally far higher than fluorescent displacement assays.[93-94]

In 2020, Synnott and colleagues showed, using SPR, that **COTI-2** may be able to interact with both full-length $p53_{R273C}$ and DBD_{R273C} —though with K_d values on the order of 10^{-6} M.[55] The SPR data is not as noise-free as one would want, and this is a very low affinity for a drug that is proposed to work at concentrations of 10^{-9} M. This K_d is also far higher than the zinc-binding affinity of **COTI-2**. It consequently seems unlikely that the actual intracellular drug is **COTI-2**. It is far more likely that it is **Zn(COTI-2)$_2$**.

$p53_{WT}$ has a zinc affinity lower than 10^{-10} M, which is the limit of detection for many extant methods. DBD_{R175H} has an affinity of approximately 2×10^{-9} M for zinc, although a second, non-native binding value of 10^{-6} M was also measured; zinc levels above this point are expected to lead to misfolding as well due to reorganization around this second site.[61] These affinities are on the same order, but slightly tighter, than the zinc affinity of the two synthetic zinc metallochaperones. There is a lot of zinc inside cells: 200 μM,[95] but it is quantitatively tied up by strong zinc binders, like $p53_{WT}$, with K_ds generally on the order of 10^{-11} M (10 pM).[96] Furthermore, cells generally keep approximately 30 μM of excess high-zinc binding ligands available.[97] This keeps free intracellular zinc concentrations at the order of 1–100 pM—these parameters imply that p53 zinc-binding mutants are generally present in their zinc-free *apo* state.[97] This naturally leads to an unfolding of the two key loops in the DBD, and in turn leads to a loss of function.

The extracellular available zinc concentration is far higher—on the order of 12-16 μM, mostly loosely bound to albumin. This acts as a reservoir, but it can be (intentionally) difficult for cells to import this zinc into the cells; **COTI-2** might be able to facilitate this transfer.

With all this circumstantial evidence for zinc binding, it is surprising that zinc binding has not been previously implicated in **COTI-2**'s mechanism of action. This is not because it hasn't been considered: in 2019 Lindemann demonstrated that **COTI-2** exerts negligible influence upon intracellular zinc levels in several HNSCC-mutant *Tp53* cells. They proposed that this meant that **COTI-2** either had low affinity for zinc, or that its mechanism of action in HNSCC cells was independent of zinc binding.[49] However, the mutants examined were DNA-contact mutants, which would have an intact zinc-binding site. We know that the issue isn't low zinc affinity, but it is still possible that **Zn(COTI-2)$_2$** would have poor cellular permeability (or retention) in this line and so may not be effective. Consequently, we wanted to examine **COTI-2**'s impact on the KLE cell line expressing $Tp53_{R175H}$ whose gene product has compromised zinc binding.

Zn(COTI-2)$_2$ is cytotoxic against human cancer cell lines.

For the reasons discussed above, we believe the active drug is not **COTI-2** but rather **Zn(COTI-2)$_2$**, as this would spontaneously form in the zinc-rich extracellular environment, readily stripping zinc from serum albumin. If this is the case, we would expect that the **Zn(COTI-2)$_2$** complex premade, would have similar cytotoxicity to the monomer **COTI-2**, as this supposes that the observed cytotoxicity of the supposed monomer has rather been due to the cytotoxicity of the zinc-mediated dimer all along. Most MTT assays are conducted with cells grown in typical media, and that media includes zinc, so we would expect this effect to be observed even in *in vitro* assays. The same cell lines that were used for the monomer were treated with the metal complex (**Figure**). The IC_{50} for the complex is lower than for the monomer for cell lines with *Tp53*$_{R175H}$—the zinc-binding mutants. It is a bit higher for the other p53 isoforms (including wildtype), but all these differences are small. This similarity in complex and monomer activity corroborates the results demonstrated with **ZMC1**; in that case, the preformed **Zn(ZMC1)$_2$** complex was observed to be modestly more active in *in vivo* models than the monomer.[61-62] This result also corroborates a zinc-driven mechanism over direct interaction: if the action of **COTI-2** was independent of metal-binding, but rather due to direct target engagement, one would expect the shape of the dimer to be considerably different than the monomer, and so one would expect a significant change in efficacy. This is not what we see. However, as suggestive as this data is, it does not prove that action is through zinc binding, or even through the dimer. We need to demonstrate zinc metallochaperone activity and show evidence that zinc-complexation is required for **COTI-2** activity. It is to these two questions that we next turned our attention.

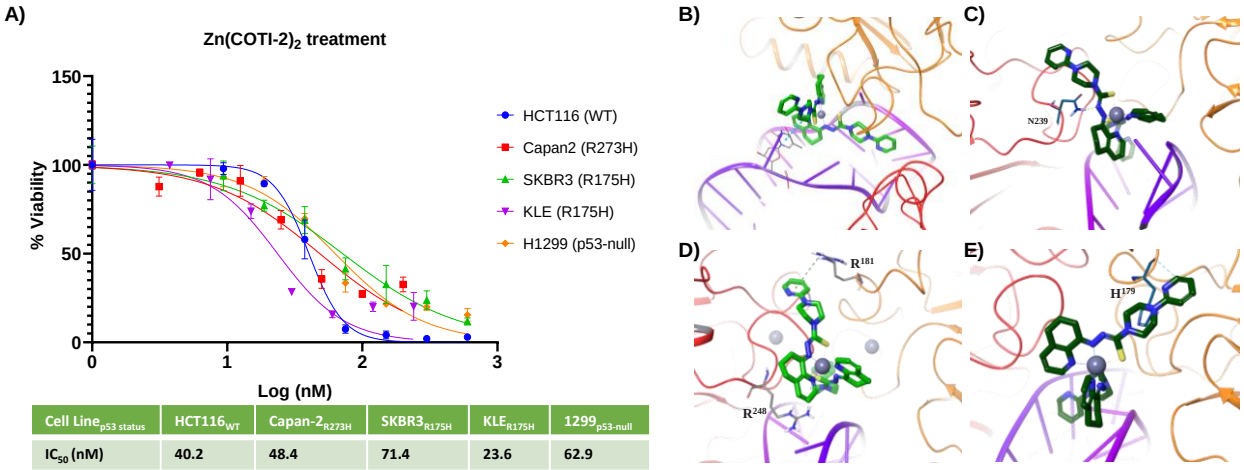

Cell Line$_{p53\ status}$	HCT116$_{WT}$	Capan-2$_{R273H}$	SKBR3$_{R175H}$	KLE$_{R175H}$	1299$_{p53\text{-}null}$
IC_{50} (nM)	40.2	48.4	71.4	23.6	62.9

Figure 6. A) The cytotoxicity of **Zn(COTI-2)$_2$** on human cancer cell lines, and its predicted binding at **Site-1**. **A)** Cytotoxicity graph for the complex. IC_{50} values were determined from maximum and minimum inhibition values and provided below the graph for reference at nanomolar concentrations. Viability values were determined from three technical replicates (mean ± SD, n=3); Predicted binding mode of **Zn(COTI-2)$_2$** with **B) WT-Zn**, **C) WT-noZn**, **D**) **R175H-Zn** & **E) R175H-noZn** at **Site-1**. Colors: **COTI-2** (green in structures with Zn, and dark green in structures without Zn), H-bond (yellow dash), π-cation (dark-green dashed), p53 units A (orange), B (red) and DNA (purple).

There is no computational evidence for a strong association between Zn(COTI-2)$_2$ and Tet-p53

If **Zn(COTI-2)$_2$** is the drug, then the poor affinity of **COTI-2** for Tet-p53 discussed above is moot. Using the same model, it is clear that **Site-1** is sufficiently large and oriented to accept the zinc complex; our model predicts that one unit of **Zn(COTI-2)$_2$** sits in a similar orientation to **COTI-2** between p53 monomers A and B (with a bias to stronger interactions with A) while also anchoring to the DNA in all of **WT-Zn**, **WT-noZn**, **R175H-Zn**, **R175H-noZn**, **R273H-Zn** and **R273H-noZn** structures with docking scores of −5.32 and −9.75, −4.31, −6.85, −5.52 and −4.72 kcal/mol, respectively (**Table S1**). In all these structures, **Zn(COTI-2)$_2$** forms an exclusively hydrophobic interface with both the DNA and units A and B as the hydrophilic side of the molecule is tied up in interacting with the zinc ion. Notably, it engages in an H-bond interaction with N^{239} of unit B for **WT-noZn**, a π-cation with R^{181} of unit A and a salt bridge with R^{248} of unit-B at **R175H-Zn** and an aromatic H-bond interaction with H^{179} of unit-A at **R175H-noZn** (**Figure 6B-E**). However, like for **COTI-2**, none of these affinities are consistent with a strong direct interaction explanatory of nM activity. It appears unlikely that even the large **Zn(COTI-2)$_2$** functions through a direct interaction with Tet-p53; the mechanism of action likely lies elsewhere. However, these interactions, especially with the zinc-free structures, could lead to a transient interaction that could help co-localize **Zn(COTI-2)$_2$** or **COTI-2** with Tet-p53; metallochaperone activity is certainly feasible.

COTI-2 and Zn(COTI-2)$_2$ increase the intracellular zinc concentration in select cell lines, acting as cell-specific zinc metallochaperones

If direct interaction is not implicated, then zinc transport and localization might be. The ionophoric features of **COTI-2** were evaluated using the FluoZin-3-AM zinc indicator in a flow cytometry assay.[98-99] **ZMC1** was employed as a positive control as it has been used in this assay before.[49] The potent zinc chelator *N,N,N′,N′*-tetrakis(2-pyridinylmethyl)-1,2-ethanediamine (TPEN) was used a negative control.[100-101] The flow cytometry analysis was performed to observe changes in fluorescence levels within cells upon KLE[102] exposure to **ZMC1** and **COTI-2** alone, or in conjunction with $Zn(NO_3)_2$ and/or TPEN. The TPEN concentration was carefully maintained to prevent any adverse effects on cell viability, and it successfully sequestered all zinc ions without showing any toxic effect on the cells. The addition of **COTI-2** and zinc to the samples led to noticeable alterations in fluorescence emission, demonstrating their influence on the zinc-oriented FluoZin fluorescence (**Figure 7**). The control group showed signs of background fluorescence, which might be attributed to the media conditions used previously. Cells were treated with either 1 μM **COTI-2** or **ZMC1**, in combination with 0.5 μM $Zn(NO_3)_2$, maintaining the same 1:2 zinc-to-drug ratio as in previous research.[49] To evaluate the effectiveness of FluoZin fluorescence, we conducted an immunofluorescence experiment (**Figure S10**).

Compared to the control, treatment with **COTI-2** alone led to a significant increase in the percentage of FluoZin+ cells, whereas established metallochaperone **ZMC1** showed a smaller increase ($p < 0.05$). In these cases, there is plenty of zinc in the media that could be captured by the drugs. **ZMC1** did elicit a considerable increase in intracellular zinc levels when administered in combination with exogenous zinc, but the absolute effect was still lower than for **COTI-2** (**Figure 7G**, **Figure S11a** & **b**).

Alongside this *Tp53*$_{R175H}$ mutant cell line (KLE) where we saw a significant effect upon introduction of **COTI-2**, we also investigated the p53$_{R273H}$ mutant-expressing Capan-2 cell line[103] to understand if there is any difference between structural and DNA-contact mutants intracellular zinc levels when **COTI-2** is applied to those cell lines.[49] Our results for this line corroborated the work of Lindeman, in that the FluoZin+ cell percentage remained unchanged when **COTI-2** was applied to Capan-2 cells, while **ZMC1** treatment caused a significant increase in the cell percentage (**Figure S12**). This is extremely curious in that there is no clear mechanism by which *Tp53* status should determine **COTI-2** internalization or efflux rates. It is also notable that this cell-line specific effect is not observed for **ZMC1**. This difference could correlate with why

COTI-2 is well tolerated in patients while **ZMC1** is not.[104] Further studies are underway to better delineate the causes and impact of this result and explore additional cell lines.

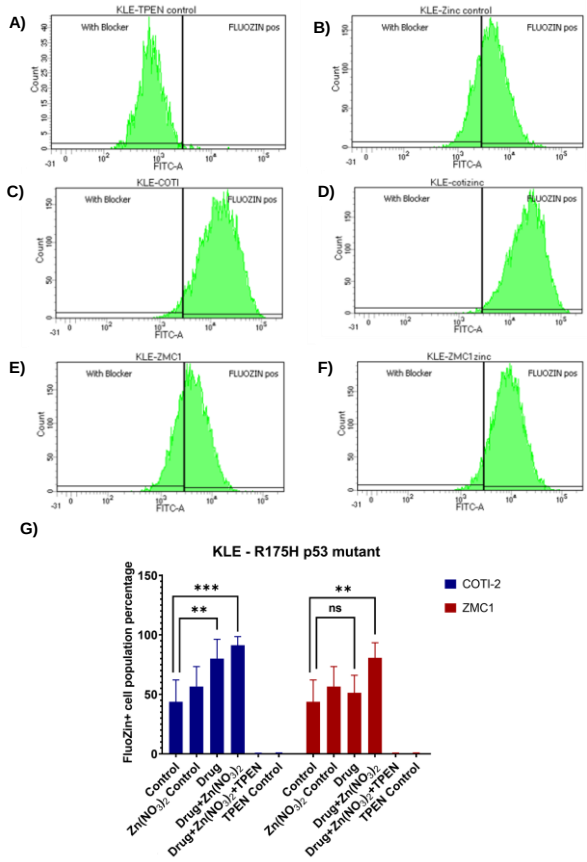

Figure 7. COTI-2 affects the intracellular zinc concentration of KLE cells. Intracellular zinc levels were assessed through flow cytometry analysis in the presence of FluoZin-3-AM. **A)** TPEN, a zinc blocker, was used as a negative control. $Zn(NO_3)_2$ served as a positive control **(B)** for zinc uptake. $Tp53_{R175H}$ KLE cells were subjected to treatment with either **COTI-2 (C)** or **ZMC1 (E)** and in the presence of $Zn(NO_3)_2$ **(D** & **F)**. The level of FluoZin+ cells was determined using a BD LSR Fortessa™ X-20 using the ratio of the wavelengths at 494/516 nm. This image illustrates the gating strategy and thresholds and was replicated in at least three independent experiments from separate subcultures. **(G)** The $p53_{R175H}$ mutant KLE cells were treated with either 1 µM of **COTI-2** or **ZMC1** in the presence of 0.5 µM of $Zn(NO_3)_2$ and/or TPEN. The graph displays the FluoZin+ cell population percentages from the flow data. A representative graph was used to depict the result of the gating procedure. Mean ± SD was derived from three separate experiments conducted independently ($p > 0.05$ non-significant, $p < 0.01$ **, $p < 0.001$ ***).

Inhibiting COTI-2's zinc binding abrogates biological activity

Based on all this information, we propose that **COTI-2** is a modulator of p53 protein function but works through a zinc-transport mechanism. If this is the case, then should the zinc-binding of **COTI-2** be abrogated, but the structure otherwise unaffected, then we should observe a decrease in activity. If the structure bound to the p53 and restored activity by inducing protein conformational change, there would be no change in the cytotoxicity. Changing the structure (to remove zinc binding) without changing the structure (geometry of the molecule) is of course impossible to do biochemically but is feasible chemically: should a metal ion of superior binding affinity in comparison to zinc occupy **COTI-2**'s metal chelation zinc-binding site, it would retain the same shape as the zinc chelate, but prevent zinc association, and consequently neutralize **COTI-2**'s ability to transport and chaperone zinc.

Zinc, cadmium, and mercury, classified as soft metals within the same group of the periodic table, exhibit a propensity to assume 2^+ oxidation states and form octahedral geometries with ligands.[105] In a study comparing the affinity of a peptide ligand for the three metals, it was shown that mercury (II) possesses the capacity to wholly displace zinc (II), while cadmium (II) exhibits the capability to partially supplant zinc (II) in complex ligand structures.[106]

Consequently, we optimized the geometry for **Zn(COTI-2)$_2$**, **Cd(COTI-2)$_2$**, and **Hg(COTI-2)$_2$** using DFT to determine the ligand dissociation energies (LDE, ΔG, **Table S3**). The average Zn-N and Zn-S bond distance from 2.14 and 2.45 Å in **Zn(COTI-2)$_2$** changed to 2.45 & 2.78 Å in **Cd(COTI-2)$_2$** and 2.58 & 2.69 Å in **Hg(COTI-2)$_2$**. When we ran the calculations, zinc also proved to have the strongest affinity. Working through the periodic table, we identified ruthenium (II) as a promising ion, with a predicted LDE of **Ru(COTI-2)$_2$** being 111.3 Kcal/mol compared to 73.4 Kcal/mol for **Zn(COTI-2)$_2$**—Ru(II) has a far higher affinity for **COTI-2** than Zn(II). Following synthesis, we confirmed this theoretical result with isothermal titration calorimetry (**Figure S9B**). The ITC result shows extremely strong binding, with a K_d below the limit of the instrument (1 nM). This is far stronger than that observed for zinc (66 nM, **Table S3, Figure S9A**).

The **COTI-2** complex with Ru^{2+} was synthesized by treating 2 equivalents of **COTI-2** with one equivalent of $RuCl_2(DMSO)_4$ in methanol under N_2. The first derivative EPR spectrum was broad with a number of poorly resolved shoulders (**Figure S32a**). These were much better resolved in the second derivative EPR spectrum (**Figure S32b**). Approaches to try and simulate the EPR spectrum as a single rhombic species ($g_x \neq g_y \neq g_z$) failed to replicate all the experimental features

but a more satisfactory simulation could be achieved using two rhombic species with an approximate ratio of 19:7 (**Figure S32c**). Both sets of EPR spectra were consistent with octahedral low spin Ru(III) ($g_z > g_y > 2.0 > g_x$) with small distortions of the coordination environment. In contrast, Ru(II) typically exhibits a $4d^6$ configuration instead of $4d^5$ and is EPR inactive in its low-spin state. Therefore, the observed EPR features strongly suggest that at least some of the complex under investigation is in the Ru(III) oxidation state, and it is inseparable from the Ru(II) species present. The nature of the oxidation state is likely moot as both the Ru(II) and Ru(III) complexes are predicted to adopt the same octahedral geometry (although the Ru(III) species would require an additional charge-stabilizing counterion and may therefore affect its ability to pass through the cell membrane). This same sample paramagnetism broadens the NMR spectrum making it impossible to differentiate multiplicities, however the chemical shifts of the spectrum are consistent with a symmetric **COTI-2** species in complex with a metal ion. The bond dissociation ΔG values for the Ru(III) **[Ru(COTI-2)$_2$]$^+$** complex have been calculated, obtaining 107.09 kcal/mol, very similar to the 111 kcal/mol of the Ru(II) species; the partial oxidation is irritating, but consequently is not a problem for this tool compound. We want to emphasize that this molecule's geometry is the same as the zinc complex but simply lacks an ability to chaperone zinc as ruthenium coordination is essentially irreversible.

The cytotoxic effectiveness of the synthesized **Ru(COTI-2)$_2$** complex was assessed through an MTT assay across multiple cell lines(

Figure A). We see no toxicity until levels reach the mid micromolar concentrations (

Figure B). It is two orders of magnitude less toxic than **Zn(COTI-2)$_2$** or **COTI-2** itself, despite ruthenium being a well-established toxin.[107] This result is precisely what we would anticipate if **COTI-2** acts through a zinc metallochaperone mechanism, and is inconsistent with a direct p53-binding refolding mechanism.

Of course, if **Ru(COTI-2)$_2$** interrupts zinc transport, we should see no increase in intracellular zinc levels, in contrast to what was seen for **COTI-2**; this is precisely what we observe (**Figures S11** & **S12**).

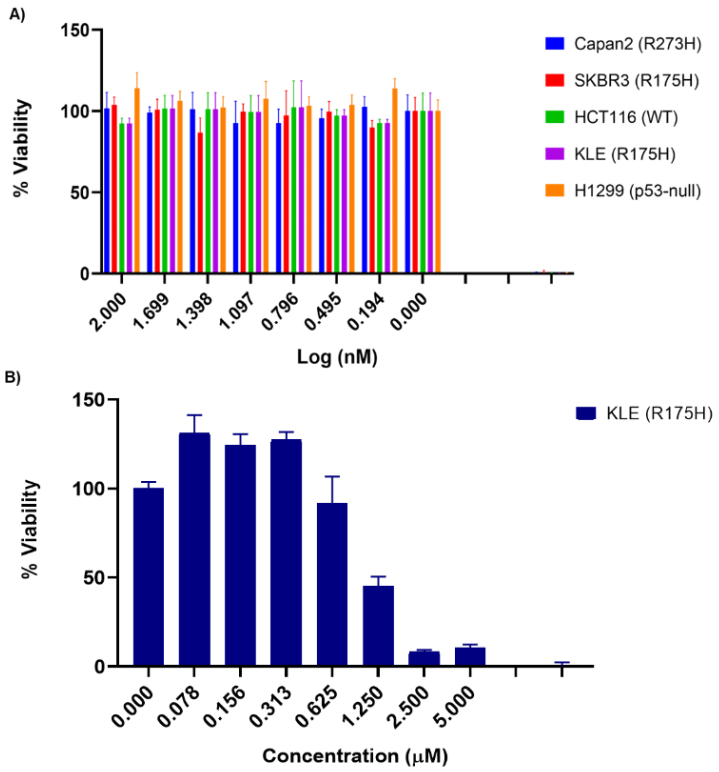

Figure 8. Ru(COTI-2)$_2$ is far less cytotoxic than Zn(COTI-2)$_2$. Cell viability percentages were measured for **(A)** various cancer cell lines at low nM concentration and **(B)** for the KLE cancer cell line at higher, μM concentrations. The x-axis is logarithmic. Data for (A) is derived from three biological replicates collected on separate days from separate subcultures, each collected in three technical replicates (mean ± SD, n=9), the data for (B) from three technical replicates (mean ± SD, n=3).

Discussion

COTI-2 has established single-digit nM efficacy against various human cancer cell lines and yet has proven to be safely non-toxic in *in vivo* models and is tolerated by patients in ongoing Phase 1b clinical trials; however, its precise mechanism of action remains unclear. It appears that it acts through p53, and through restoring function to certain p53 mutants, but it is also generally considered that it has additional modes of action. A zinc metallochaperone role has been previously

dismissed based on experimental studies.[49] This leaves its possible mode of action to be thought to be some form of direct binding and induced refolding of the mutant.

The current work contradicts this hypothesis. The evidence presented here is that despite our best efforts, neither experimental nor theoretical models could establish any evidence of potent target engagement one would expect to see for a direct binder functional at single digit nM concentrations. We also conclusively demonstrate that **COTI-2** unambiguously binds to Zn^{2+} with exceptional affinity. Application of the **Zn(COTI-2)$_2$** premade complex results in cytotoxicity data similar, and in most cases slightly improved, than for **COTI-2** alone. The basic fact of zinc concentration *in vivo* coupled with **COTI-2**'s zinc affinity makes it unlikely that **COTI-2** exists as a free monomer in solution; it binds zinc and may make a dimer with another **COTI-2** ligand or possibly another set of endogenous biological ligands. We note that **Ru(COTI-2)$_2$**, with the same shape and geometry as **Zn(COTI-2)$_2$**, had greatly diminished (by approximately two to three orders of magnitude) cytotoxicity. Similarly, supplementing zinc-binding mutants of p53 with extraneous zinc does increase cytotoxicity, although to a lesser extent than adding **COTI-2**.[4] Zinc ions do not readily pass freely through the cellular membrane, and mammalian cells, although bathed in a relatively zinc-rich extracellular environment *in vivo*, maintain a very small zinc reservoir within the cells; consequently, simple increase in extracellular zinc concentration without a mechanism of transporting the zinc into the cells provides little effect. This is essential as zinc homeostasis must be tightly controlled within cells[97]—this is after all why zinc metallochaperones can be toxic.[25, 108]

We note that the systemically toxic zinc metallochaperone **ZMC1** increased the intracellular zinc concentration in the cell lines examined in line with previous reports of the molecule. **COTI-2**, which shares the same zinc binding motif, and has a similar affinity for zinc, does not increase the zinc concentration in all cells examined. It appears to have a different cell distribution profile to **ZMC1.** This likely arises from specific structural effects that control **COTI-2**'s efflux and ingress into cells, and this differential behaviour is likely correlated with the observation that it is tolerated by humans and can be used as a treatment, while **ZMC1** has a far narrower therapeutic window. It is important to note that simply because **COTI-2** does not increase the intracellular zinc levels inside Capan-2 cells, for example, does not mean that it is not acting as a zinc metallochaperone for those cells (after all, it remains highly cytotoxic against the line), simply that it is not accumulating zinc inside the cells. High resolution mass spectrometric **COTI-**

2 localization studies are currently underway in our lab to better understand the distribution of the drug in different cell lines and will be reported on in due course.

Furthermore, seeing that it has very potent activity in a p53-null cell line shows that **COTI-2**'s effect is not p53-specific—many other proteins bind to zinc, and many other processes are mediated by these proteins. Of course, even if **COTI-2** interacts through a zinc metallochaperone effect, this does not preclude other mechanisms of action. This is consistent with Lindemann *et al.'s* findings which further suggest that **COTI-2**'s action in HNSCC cells might operate independently from zinc chelation.[49] More thorough structural biology, biophysics, structure activity relationship, molecular biology, and interactome studies are currently underway in our lab to better understand these other modes of action.

Conclusion

COTI-2 is a very potent, but still well-tolerated, anticancer agent that acts, at least partially, through restoring function to specific p53 mutants. The evidence does not support that this activity arises from a physical binding and refolding of the inactive mutants, but rather through the colocalization and deliverance of zinc to mutants that might have lost their ions. This still induces a refolding of the mutant to the wild-type conformation, but indirectly rather than directly. This is remarkable as unlike other zinc metallochaperones that are not tolerated in patients as they disrupt zinc homeostasis more generally in all cells, our preliminary analysis shows that **COTI-2** does not affect all cell lines. This might underlie its expanded therapeutic window. It is also clear that zinc-mediation and/or p53 activity are not the only mechanisms of action for this small molecule, and other effects are simultaneously active that help define its remarkable biological activity. As p53 mutants are found in the plurality of cancers, and as there are no approved therapies that engage and restore proper function to this protein, **COTI-2** deserves special attention. Likewise, although refolding misfolded proteins is an extremely difficult challenge, misfolding can arise from multiple causes, and restoring the proper binding of cofactors can be a feasible way to restore malfunctioning proteins to their proper conformation.

Supporting Information

The supporting information accompanying the article includes full experimental details for the synthesis of **COTI-2**, **[Zn(COTI-2)$_2$]**, and **[Ru(COTI-2)$_2$]**. It also includes additional figures as

referenced in the text for the biological assay data, computational analyses, and biophysical measurements. All computational structures discussed in the article are available on the Borealis Dataverse (Borealisdata.ca), a repository jointly operated by the Canadian Universities and Research Institutes at https://doi.org/10.5683/SP3/RENQVK.

Author Contributions

Conceptualization, JFT, FSR, RH; Funding acquisition JFT; Investigation — Biology, IS, AD, DA; Investigation — Chemistry and characterization, MJK, PX, SK, OT, KB, JJH; Investigation — *in silico* analysis, FSR, AM, MK, FP; Methodology, IS, FSR, RH, JFT; Visualization, FSR, IS, MK, SK; Project administration, JFT, FSR; Supervision, JFT; Writing original draft, IS, FSR, PX, JFT; Writing–review and editing, All authors.

Conflict of Interest Statement

Cotinga holds patents (WO2008083491, US8822475B2) on **COTI-2**. Cotinga was involved with planning the initial direction of this research, but had no input into the specific methodologies employed, nor did they have any input or access to limit or influence the results or conclusions of the work. Cotinga was provided with a draft of the manuscript prior to submission. Cotinga did not provide funding to support this work. IP generated from these results, although potentially of value to Cotinga, is owned by Dr. Trant as per the University of Windsor Faculty Agreement and has not been transferred to Cotinga or any other party as of the submission of this manuscript.

JFT and FSR are associated with Binary Star Research Services (BSRS). BSRS has not had input into this project and has no commercial interests in the subject of this work. BSRS holds no IP on this project, nor did it provide or receive any funding associated with this work.

RH is associated with Amaro Therapeutics. Amaro had no input into this study and has no business interest in COTI-2, oncology, or p53-related therapeutics. RH's involvement is independent and not associated with his role at Amaro.

Acknowledgements

The authors would like to thank the Natural Sciences and Engineering Research Council of Canada (2018-06338, ALLRP- 555689-20) for funding support. FSR, AM, MK, and JFT wish

to recognize that this work was made possible by the facilities of Compute Ontario (https://www.computeontario.ca) and the Digital Research Alliance of Canada (www.alliancecan.ca).

Uncategorized References

1. Hassin, O.; Oren, M., Drugging p53 in cancer: One protein, many targets. *Nat. Rev. Drug Discov.* **2023,** *22* (2), 127-144.
2. Feroz, W.; Sheikh, A. M. A., Exploring the multiple roles of guardian of the genome: p53. *Egypt. J. Med. Hum. Genet.* **2020,** *21* (1), 49.
3. Kastan, M. B., Wild-type p53: Tumors can't stand it. *Cell* **2007,** *128* (5), 837-40.
4. Chène, P., The role of tetramerization in p53 function. *Oncogene* **2001,** *20* (21), 2611-2617.
5. Nicholls, C. D.; McLure, K. G.; Shields, M. A.; Lee, P. W. K., Biogenesis of p53 involves cotranslational dimerization of monomers and posttranslational dimerization of dimers: Implications on the dominant negative effect. *J. Biol. Chem.* **2002,** *277* (15), 12937-12945.
6. Duffy, M. J.; Synnott, N. C.; Crown, J., Mutant p53 as a target for cancer treatment. *Eur. J. Cancer* **2017,** *83*, 258-265.
7. Alvarado-Ortiz, E.; de la Cruz-López, K. G.; Becerril-Rico, J.; Sarabia-Sánchez, M. A.; Ortiz-Sánchez, E.; García-Carrancá, A., Mutant p53 gain-of-function: Role in cancer development, progression, and therapeutic approaches. *Front. Cell Dev. Biol.* **2020,** *8*, 607670.
8. Wang, H.; Guo, M.; Wei, H.; Chen, Y., Targeting p53 pathways: Mechanisms, structures, and advances in therapy. *Signal Transduct. Target Ther.* **2023,** *8* (1), 92.
9. Kandoth, C.; McLellan, M. D.; Vandin, F.; Ye, K.; Niu, B.; Lu, C.; Xie, M.; Zhang, Q.; McMichael, J. F.; Wyczalkowski, M. A.; Leiserson, M. D. M.; Miller, C. A.; Welch, J. S.; Walter, M. J.; Wendl, M. C.; Ley, T. J.; Wilson, R. K.; Raphael, B. J.; Ding, L., Mutational landscape and significance across 12 major cancer types. *Nature* **2013,** *502* (7471), 333-339.
10. Kennedy, M. C.; Lowe, S. W., Mutant p53: It's not all one and the same. *Cell Death Differ.* **2022,** *29* (5), 983-987.
11. Bykov, V. J. N.; Eriksson, S. E.; Bianchi, J.; Wiman, K. G., Targeting mutant p53 for efficient cancer therapy. *Nat. Rev. Cancer* **2018,** *18* (2), 89-102.
12. Tisato, V.; Voltan, R.; Gonelli, A.; Secchiero, P.; Zauli, G., MDM2/X inhibitors under clinical evaluation: Perspectives for the management of hematological malignancies and pediatric cancer. *J. Hematol. Oncol.* **2017,** *10* (1), 133.
13. Gupta, A.; Shah, K.; Oza, M. J.; Behl, T., Reactivation of p53 gene by MDM2 inhibitors: A novel therapy for cancer treatment. *Biomed. Pharmacother.* **2019,** *109*, 484-492.
14. Burgess, A.; Chia, K. M.; Haupt, S.; Thomas, D.; Haupt, Y.; Lim, E., Clinical overview of MDM2/X-targeted therapies. *Front. Oncol.* **2016,** *6*, 7.
15. Ray-Coquard, I.; Blay, J. Y.; Italiano, A.; Le Cesne, A.; Penel, N.; Zhi, J.; Heil, F.; Rueger, R.; Graves, B.; Ding, M.; Geho, D.; Middleton, S. A.; Vassilev, L. T.; Nichols, G. L.; Bui, B. N., Effect of the MDM2 antagonist RG7112 on the p53 pathway in patients with MDM2-amplified, well-differentiated or dedifferentiated liposarcoma: an exploratory proof-of-mechanism study. *Lancet Oncol.* **2012,** *13* (11), 1133-40.
16. Liguori, L.; Monticelli, M.; Allocca, M.; Hay Mele, B.; Lukas, J.; Cubellis, M. V.; Andreotti, G., Pharmacological chaperones: A therapeutic approach for diseases caused by destabilizing missense mutations. *Int. J. Mol. Sci.* **2020,** *21* (2), 489.
17. Duffy, M. J.; Synnott, N. C.; O'Grady, S.; Crown, J., Targeting p53 for the treatment of cancer. *Semin. Cancer Biol.* **2022,** *79*, 58-67.
18. Blanden, A. R.; Yu, X.; Blayney, A. J.; Demas, C.; Ha, J. H.; Liu, Y.; Withers, T.; Carpizo, D. R.; Loh, S. N., Zinc shapes the folding landscape of p53 and establishes a pathway for reactivating structurally diverse cancer mutants. *eLife* **2020,** *9*.
19. Ha, J. H.; Prela, O.; Carpizo, D. R.; Loh, S. N., p53 and Zinc: A malleable relationship. *Front. Mol. Biosci.* **2022,** *9*, 895887.

20. Yu, X.; Carpizo, D. R., Flipping the “switch” on mutant p53 by zinc metallochaperones: how a brief pulse of zinc can reactivate mutant p53 to kill cancer. *Oncotarget* **2019,** *10* (9), 918-919.
21. Baugh, E. H.; Ke, H.; Levine, A. J.; Bonneau, R. A.; Chan, C. S., Why are there hotspot mutations in the Tp53 gene in human cancers? *Cell Death Differ.* **2018,** *25* (1), 154-160.
22. Gomes, A. S.; Ramos, H.; Inga, A.; Sousa, E.; Saraiva, L., Structural and drug targeting insights on mutant p53. *Cancers (Basel)* **2021,** *13* (13).
23. Chiang, Y. T.; Chien, Y. C.; Lin, Y. H.; Wu, H. H.; Lee, D. F.; Yu, Y. L., The function of the mutant p53-R175H in cancer. *Cancers (Basel)* **2021,** *13* (16).
24. Li, L.; Li, X.; Tang, Y.; Lao, Z.; Lei, J.; Wei, G., Common cancer mutations R175H and R273H drive the p53 DNA-binding domain towards aggregation-prone conformations. *Phys. Chem. Chem. Phys.* **2020,** *22* (17), 9225-9232.
25. Kogan, S.; Carpizo, D. R., Zinc metallochaperones as mutant p53 reactivators: A new paradigm in cancer therapeutics. *Cancers (Basel)* **2018,** *10* (6).
26. Annor, G. K.; Elshabassy, N.; Lundine, D.; Conde, D. G.; Xiao, G.; Ellison, V.; Bargonetti, J., Oligomerization of mutant p53 R273H is not required for gain-of-function chromatin associated activities. *Front. Cell Dev. Biol.* **2021,** *9*, 772315.
27. Oren, M.; Rotter, V., Mutant p53 gain-of-function in cancer. *Cold Spring Harb. Perspect. Biol.* **2010,** *2* (2), a001107.
28. Stein, Y.; Rotter, V.; Aloni-Grinstein, R., Gain-of-function mutant p53: All the roads lead to tumorigenesis. *Int. J. Mol. Sci.* **2019,** *20* (24), 6197.
29. Thayer, K. M.; Stetson, S.; Caballero, F.; Chiu, C.; Han, I. S. M., Navigating the complexity of p53-DNA binding: Implications for cancer therapy. *Biophys. Rev.* **2024**.
30. Liu, X.; Wilcken, R.; Joerger, A. C.; Chuckowree, I. S.; Amin, J.; Spencer, J.; Fersht, A. R., Small molecule induced reactivation of mutant p53 in cancer cells. *Nucleic Acids Res.* **2013,** *41* (12), 6034-44.
31. Wilcken, R.; Liu, X.; Zimmermann, M. O.; Rutherford, T. J.; Fersht, A. R.; Joerger, A. C.; Boeckler, F. M., Halogen-enriched fragment libraries as leads for drug rescue of mutant p53. *J. Am. Chem. Soc* **2012,** *134* (15), 6810-6818.
32. Wassman, C. D.; Baronio, R.; Demir, Ö.; Wallentine, B. D.; Chen, C.-K.; Hall, L. V.; Salehi, F.; Lin, D.-W.; Chung, B. P.; Wesley Hatfield, G.; Richard Chamberlin, A.; Luecke, H.; Lathrop, R. H.; Kaiser, P.; Amaro, R. E., Computational identification of a transiently open L1/S3 pocket for reactivation of mutant p53. *Nat. Commun.* **2013,** *4* (1), 1407.
33. Pradhan, M. R.; Siau, J. W.; Kannan, S.; Nguyen, M. N.; Ouaray, Z.; Kwoh, C. K.; Lane, D. P.; Ghadessy, F.; Verma, C. S., Simulations of mutant p53 DNA binding domains reveal a novel druggable pocket. *Nucl. Acids Res.* **2019,** *47* (4), 1637-1652.
34. Foster, B. A.; Coffey, H. A.; Morin, M. J.; Rastinejad, F., Pharmacological rescue of mutant p53 conformation and function. *Science* **1999,** *286* (5449), 2507-2510.
35. Zache, N.; Lambert, J. M. R.; Rökaeus, N.; Shen, J.; Hainaut, P.; Bergman, J.; Wiman, K. G.; Bykov, V. J. N., Mutant p53 targeting by the low molecular weight compound STIMA-1. *Mol. Oncol.* **2008,** *2* (1), 70-80.
36. Bykov, V. J. N.; Issaeva, N.; Shilov, A.; Hultcrantz, M.; Pugacheva, E.; Chumakov, P.; Bergman, J.; Wiman, K. G.; Selivanova, G., Restoration of the tumor suppressor function to mutant p53 by a low-molecular-weight compound. *Nat. Med.* **2002,** *8* (3), 282-288.
37. Shah, H. D.; Saranath, D.; Murthy, V., A molecular dynamics and docking study to screen anti-cancer compounds targeting mutated p53. *J. Biomol. Struct. Dyn.* **2022,** *40* (6), 2407-2416.
38. Parrales, A.; Iwakuma, T., Targeting oncogenic mutant p53 for cancer therapy. *Front. Oncol.* **2015,** *5*, 288.
39. Duffy, M. J.; Crown, J., Drugging “undruggable” genes for cancer treatment: Are we making progress? *Int. J. Cancer* **2021,** *148* (1), 8-17.

40. Aguilar, A.; Wang, S., Therapeutic strategies to activate p53. *Pharmaceuticals* **2023,** *16* (1), 24.
41. Birsen, R.; Larrue, C.; Decroocq, J.; Johnson, N.; Guiraud, N.; Gotanegre, M.; Cantero-Aguilar, L.; Grignano, E.; Huynh, T.; Fontenay, M.; Kosmider, O.; Mayeux, P.; Chapuis, N.; Sarry, J. E.; Tamburini, J.; Bouscary, D., APR-246 induces early cell death by ferroptosis in acute myeloid leukemia. *Haematologica* **2022,** *107* (2), 403-416.
42. Freed-Pastor, W. A.; Prives, C., Mutant p53: One name, many proteins. *Genes Dev.* **2012,** *26* (12), 1268-86.
43. Duffy, M. J.; Tang, M.; Rajaram, S.; O'Grady, S.; Crown, J., Targeting mutant p53 for cancer treatment: Moving closer to clinical use? *Cancers (Basel)* **2022,** *14* (18).
44. Degtjarik, O.; Golovenko, D.; Diskin-Posner, Y.; Abrahmsén, L.; Rozenberg, H.; Shakked, Z., Structural basis of reactivation of oncogenic p53 mutants by a small molecule: Methylene quinuclidinone (MQ). *Nat Commun* **2021,** *12* (1), 7057.
45. Li, X.-L.; Zhou, J.; Chan, Z.-L.; Chooi, J.-Y.; Chen, Z.-R.; Chng, W.-J., PRIMA-1met (APR-246) inhibits growth of colorectal cancer cells with different p53 status through distinct mechanisms. *Oncotarget* **2015,** *6* (34), 36689.
46. Bao, W.; Chen, M.; Zhao, X.; Kumar, R.; Spinnler, C.; Thullberg, M.; Issaeva, N.; Selivanova, G.; Stromblad, S., PRIMA-1Met/APR-246 induces wild-type p53-dependent suppression of malignant melanoma tumor growth in 3D culture and *in vivo*. *Cell Cycle* **2011,** *10* (2), 301-307.
47. Wang, Z.; Hu, H.; Heitink, L.; Rogers, K.; You, Y.; Tan, T.; Suen, C. L. W.; Garnham, A.; Chen, H.; Lieschke, E.; Diepstraten, S. T.; Chang, C.; Chen, T.; Moujalled, D.; Sutherland, K.; Lessene, G.; Sieber, O. M.; Visvader, J.; Kelly, G. L.; Strasser, A., The anti-cancer agent APR-246 can activate several programmed cell death processes to kill malignant cells. *Cell Death Differ.* **2023,** *30* (4), 1033-1046.
48. Maleki Vareki, S.; Salim, K. Y.; Danter, W. R.; Koropatnick, J., Novel anti-cancer drug COTI-2 synergizes with therapeutic agents and does not induce resistance or exhibit cross-resistance in human cancer cell lines. *PLoS ONE* **2018,** *13* (1), e0191766.
49. Lindemann, A.; Patel, A. A.; Silver, N. L.; Tang, L.; Liu, Z.; Wang, L.; Tanaka, N.; Rao, X.; Takahashi, H.; Maduka, N. K.; Zhao, M.; Chen, T.-C.; Liu, W.; Gao, M.; Wang, J.; Frank, S. J.; Hittelman, W. N.; Mills, G. B.; Myers, J. N.; Osman, A. A., COTI-2, a novel thiosemicarbazone derivative, exhibits antitumor activity in HNSCC through p53-dependent and -independent mechanisms. *Clin. Cancer Res.* **2019,** *25* (18), 5650-5662.
50. Critical Outcome Technologies Inc. A phase 1 study of COTI-2 as monotherapy or combination therapy for the treatment of advanced or recurrent malignancies; clinical trial registration NCT02433626; . https://clinicaltrials.gov/study/NCT02433626.
51. Salim, K. Y.; Maleki Vareki, S.; Danter, W. R.; Koropatnick, J., COTI-2, a novel small molecule that is active against multiple human cancer cell lines in vitro and in vivo. *Oncotarget* **2016,** *7* (27), 41363-41379.
52. Joerger, A. C.; Fersht, A. R., Structural biology of the tumor suppressor p53. *Annu. Rev. Biochem.* **2008,** *77*, 557-82.
53. Masangkay, E. G., FDA grants orphan drug status To COTI's ovarian cancer drug COTI-2. *Pharmaceutical Online,* 2014.
54. Guo, Y.; Zhu, X.; Sun, X., COTI-2 induces cell apoptosis in pediatric acute lymphoblastic leukemia via upregulation of miR-203. *Bioengineered* **2020,** *11* (1), 201-208.
55. Synnott, N. C.; O'Connell, D.; Crown, J.; Duffy, M. J., COTI-2 reactivates mutant p53 and inhibits growth of triple-negative breast cancer cells. *Breast Cancer Res. Treat.* **2020,** *179* (1), 47-56.
56. Bormio Nunes, J. H.; Hager, S.; Mathuber, M.; Pósa, V.; Roller, A.; Enyedy É, A.; Stefanelli, A.; Berger, W.; Keppler, B. K.; Heffeter, P.; Kowol, C. R., Cancer cell resistance against the clinically investigated thiosemicarbazone COTI-2 is based on formation of intracellular copper complex glutathione adducts and ABCC1-mediated efflux. *J. Med. Chem.* **2020,** *63* (22), 13719-13732.

57. Liu, D. P.; Song, H.; Xu, Y., A common gain of function of p53 cancer mutants in inducing genetic instability. *Oncogene* **2010,** *29* (7), 949-956.
58. Yu, Y.; Kalinowski, D. S.; Kovacevic, Z.; Siafakas, A. R.; Jansson, P. J.; Stefani, C.; Lovejoy, D. B.; Sharpe, P. C.; Bernhardt, P. V.; Richardson, D. R., Thiosemicarbazones from the old to new: Iron chelators that are more than just ribonucleotide reductase inhibitors. *J. Med. Chem.* **2009,** *52* (17), 5271-5294.
59. Yu, X.; Vazquez, A.; Levine, A. J.; Carpizo, D. R., Allele-specific p53 mutant reactivation. *Cancer Cell* **2012,** *21* (5), 614-625.
60. Yu, X.; Blanden, A. R.; Narayanan, S.; Jayakumar, L.; Lubin, D.; Augeri, D.; Kimball, S. D.; Loh, S. N.; Carpizo, D. R., Small molecule restoration of wildtype structure and function of mutant p53 using a novel zinc-metallochaperone based mechanism. *Oncotarget* **2014,** *5* (19), 8879-92.
61. Blanden, A. R.; Yu, X.; Wolfe, A. J.; Gilleran, J. A.; Augeri, D. J.; O'Dell, R. S.; Olson, E. C.; Kimball, S. D.; Emge, T. J.; Movileanu, L.; Carpizo, D. R.; Loh, S. N., Synthetic metallochaperone ZMC1 rescues mutant p53 conformation by transporting zinc into cells as an ionophore. *Mol. Pharmacol.* **2015,** *87* (5), 825.
62. Yu, X.; Kogan, S.; Chen, Y.; Tsang, A. T.; Withers, T.; Lin, H.; Gilleran, J.; Buckley, B.; Moore, D.; Bertino, J.; Chan, C.; Kimball, S. D.; Loh, S. N.; Carpizo, D. R., Zinc metallochaperones reactivate mutant p53 using an ON/OFF switch mechanism: A new paradigm in cancer therapeutics. *Clin. Cancer Res.* **2018,** *24* (18), 4505-4517.
63. Das, T.; Mukhopadhyay, C., Molecular dynamics simulations suggest thiosemicarbazones can bind p53 cancer mutant R175H. *Biochim. Biophys. Acta Proteins Proteom.* **2023,** *1871* (3), 140903.
64. Danter, W. R.; Brown, M.; Lepifre, F. Preparation of thiosemicarbazone derivatives for treatment of cancers. WO2008083491, 2008.
65. Danter, W. R.; Brown, M.; Lepifre, F. Compounds and method for treatment of cancer. US8822475B2, 2008.
66. Sadraei, S. I.; Yousif, G.; Taimoory, S. M.; Kosar, M.; Mehri, S.; Alolabi, R.; Igbokwe, E.; Toma, J.; Rahim, M. M. A.; Trant, J. F., The total synthesis of glycolipids from *S. pneumoniae* and a re-evaluation of their immunological activity. *ChemBioChem* **2022,** *23*, e202200361.
68. van Engeland, M.; Nieland, L. J. W.; Ramaekers, F. C. S.; Schutte, B.; Reutelingsperger, C. P. M., Annexin V-affinity assay: A review on an apoptosis detection system based on phosphatidylserine exposure. *Cytometry* **1998,** *31* (1), 1-9.
69. Jafari, R.; Almqvist, H.; Axelsson, H.; Ignatushchenko, M.; Lundbäck, T.; Nordlund, P.; Martinez Molina, D., The cellular thermal shift assay for evaluating drug target interactions in cells. *Nat. Protoc.* **2014,** *9* (9), 2100-22.
70. Molina Daniel, M.; Jafari, R.; Ignatushchenko, M.; Seki, T.; Larsson, E. A.; Dan, C.; Sreekumar, L.; Cao, Y.; Nordlund, P., Monitoring drug target engagement in cells and tissues using the cellular thermal shift assay. *Science* **2013,** *341* (6141), 84-87.
71. Dart, M. L.; Machleidt, T.; Jost, E.; Schwinn, M. K.; Robers, M. B.; Shi, C.; Kirkland, T. A.; Killoran, M. P.; Wilkinson, J. M.; Hartnett, J. R.; Zimmerman, K.; Wood, K. V., Homogeneous assay for target engagement utilizing bioluminescent thermal shift. *ACS Med. Chem. Lett.* **2018,** *9* (6), 546-551.
72. Gomes, A. S.; Ramos, H.; Gomes, S.; Loureiro, J. B.; Soares, J.; Barcherini, V.; Monti, P.; Fronza, G.; Oliveira, C.; Domingues, L.; Bastos, M.; Dourado, D.; Carvalho, A. L.; Romão, M. J.; Pinheiro, B.; Marcelo, F.; Carvalho, A.; Santos, M. M. M.; Saraiva, L., SLMP53-1 interacts with wild-type and mutant p53 DNA-binding domain and reactivates multiple hotspot mutations. *Biochim. Biophys. Acta Gen. Subj.* **2020,** *1864* (1), 129440.
73. Ramos, H.; Soares, M. I. L.; Silva, J.; Raimundo, L.; Calheiros, J.; Gomes, C.; Reis, F.; Monteiro, F. A.; Nunes, C.; Reis, S.; Bosco, B.; Piazza, S.; Domingues, L.; Chlapek, P.; Vlcek, P.; Fabian, P.; Rajado, A. T.; Carvalho, A. T. P.; Veselska, R.; Inga, A.; Pinho, E. M. T.; Saraiva, L., A selective p53 activator and anticancer agent to improve colorectal cancer therapy. *Cell Rep.* **2021,** *35* (2), 108982.

74. Ishii, T.; Okai, T.; Iwatani-Yoshihara, M.; Mochizuki, M.; Unno, S.; Kuno, M.; Yoshikawa, M.; Shibata, S.; Nakakariya, M.; Yogo, T.; Kawamoto, T., CETSA quantitatively verifies *in vivo* target engagement of novel RIPK1 inhibitors in various biospecimens. *Sci. Rep.* **2017,** *7* (1), 13000.
75. Schneider-Poetsch, T.; Ju, J.; Eyler, D. E.; Dang, Y.; Bhat, S.; Merrick, W. C.; Green, R.; Shen, B.; Liu, J. O., Inhibition of eukaryotic translation elongation by cycloheximide and lactimidomycin. *Nat. Chem. Biol.* **2010,** *6* (3), 209-217.
76. Dai, C. L.; Shi, J.; Chen, Y.; Iqbal, K.; Liu, F.; Gong, C. X., Inhibition of protein synthesis alters protein degradation through activation of protein kinase B (AKT). *J. Biol. Chem.* **2013,** *288* (33), 23875-83.
77. Drake, W. R.; Hou, C. W.; Zachara, N. E.; Grimes, C. L., New use for CETSA: Monitoring innate immune receptor stability via post-translational modification by OGT. *J. Bioenerg. Biomembr.* **2018,** *50* (3), 231-240.
78. Tian, Z.; An, N.; Zhou, B.; Xiao, P.; Kohane, I. S.; Wu, E., Cytotoxic diarylheptanoid induces cell cycle arrest and apoptosis via increasing ATF3 and stabilizing p53 in SH-SY5Y cells. *Cancer Chemother. Pharmacol.* **2009,** *63* (6), 1131-9.
79. Lubin, D. J.; Butler, J. S.; Loh, S. N., Folding of tetrameric p53: Oligomerization and tumorigenic mutations induce misfolding and loss of function. *J. Mol. Biol.* **2010,** *395* (4), 705-16.
80. D'Abramo, M.; Bešker, N.; Desideri, A.; Levine, A. J.; Melino, G.; Chillemi, G., The p53 tetramer shows an induced-fit interaction of the C-terminal domain with the DNA-binding domain. *Oncogene* **2016,** *35* (25), 3272-3281.
81. Demir, Ö.; Ieong, P. U.; Amaro, R. E., Full-length p53 tetramer bound to DNA and its quaternary dynamics. *Oncogene* **2017,** *36* (10), 1451-1460.
82. Emamzadah, S.; Tropia, L.; Halazonetis, T. D., Crystal structure of a multidomain human p53 tetramer bound to the natural CDKN1A (p21) p53-response element. *Mol. Cancer Res.* **2011,** *9* (11), 1493-1499.
83. Soares, J.; Raimundo, L.; Pereira, N. A. L.; Monteiro, Â.; Gomes, S.; Bessa, C.; Pereira, C.; Queiroz, G.; Bisio, A.; Fernandes, J.; Gomes, C.; Reis, F.; Gonçalves, J.; Inga, A.; Santos, M. M. M.; Saraiva, L., Reactivation of wild-type and mutant p53 by tryptophanolderived oxazoloisoindolinone SLMP53-1, a novel anticancer small-molecule. *Oncotarget* **2015,** *7* (4).
84. Halgren, T. A., Identifying and characterizing binding sites and assessing druggability. *J. Chem. Inf. Model.* **2009,** *49* (2), 377-389.
85. Halgren, T. A.; Murphy, R. B.; Friesner, R. A.; Beard, H. S.; Frye, L. L.; Pollard, W. T.; Banks, J. L., Glide: A new approach for rapid, accurate docking and scoring. 2. Enrichment factors in database screening. *J. Med. Chem.* **2004,** *47* (7), 1750-1759.
86. Bell, S.; Klein, C.; Müller, L.; Hansen, S.; Buchner, J., p53 contains large unstructured regions in its native state. *J. Mol. Biol.* **2002,** *322* (5), 917-927.
87. Lima, I.; Navalkar, A.; Maji, S. K.; Silva, J. L.; de Oliveira, G. A. P.; Cino, E. A., Biophysical characterization of p53 core domain aggregates. *Biochem. J.* **2020,** *477* (1), 111-120.
88. Luwang, J. W.; Nair, A. R.; Natesh, R., Stability of p53 oligomers: Tetramerization of p53 impinges on its stability. *Biochimie* **2021,** *189*, 99-107.
89. Song, B.; Wang, J.; Ren, Y.; Su, Y.; Geng, X.; Yang, F.; Wang, H.; Zhang, J., Butein inhibits cancer cell growth by rescuing the wild-type thermal stability of mutant p53. *Biomed. Pharmacother.* **2023,** *163*, 114773.
90. Choundhury, S.; Kolukula, V.; Preet, A.; Albanese, C.; avantaggiati, m., Dissecting the pathways that destabilize mutant p53: The proteasome or autophagy? *Cell Cycle* **2013,** *12* (7), 1022-1029.
91. Amaral, J. D.; Castro, R. E.; Solá, S.; Steer, C. J.; Rodrigues, C. M. P., Ursodeoxycholic acid modulates the ubiquitin-proteasome degradation pathway of p53. *Biochem. Biophys. Res. Commun.* **2010,** *400* (4), 649-654.

92. Lobana, T. S.; Sharma, R.; Bawa, G.; Khanna, S., Bonding and structure trends of thiosemicarbazone derivatives of metals—An overview. *Coord. Chem. Rev.* **2009,** *253* (7), 977-1055.
93. Hansen, L. D.; Quinn, C., Obtaining precise and accurate results by ITC. *Eur. Biophys. J.* **2019,** *48* (8), 825-835.
94. Ciulli, A., Biophysical Screening for the Discovery of Small-Molecule Ligands. In *Protein-Ligand Interactions: Methods and Applications*, Williams, M. A.; Daviter, T., Eds. Humana Press: Totowa, NJ, 2013; pp 357-388.
95. Haase, H.; Hebel, S.; Engelhardt, G.; Rink, L., The biochemical effects of extracellular Zn^{2+} and other metal ions are severely affected by their speciation in cell culture media. *Metallomics* **2015,** *7* (1), 102-111.
96. Ollig, J.; Kloubert, V.; Weßels, I.; Haase, H.; Rink, L., Parameters influencing zinc in experimental systems *in vivo* and *in vitro*. *Metals* **2016,** *6* (3), 71.
97. Colvin, R. A.; Holmes, W. R.; Fontaine, C. P.; Maret, W., Cytosolic zinc buffering and muffling: Their role in intracellular zinc homeostasis. *Metallomics* **2010,** *2* (5), 306-317.
98. Marszałek, I.; Krężel, A.; Goch, W.; Zhukov, I.; Paczkowska, I.; Bal, W., Revised stability constant, spectroscopic properties and binding mode of Zn(II) to FluoZin-3, the most common zinc probe in life sciences. *J. Inorg. Biochem.* **2016,** *161*, 107-114.
99. Carpenter, M. C.; Lo, M. N.; Palmer, A. E., Techniques for measuring cellular zinc. *Archiv. Biochem. Biophys.* **2016,** *611*, 20-29.
100. Fatfat, M.; Merhi, R. A.; Rahal, O.; Stoyanovsky, D. A.; Zaki, A.; Haidar, H.; Kagan, V. E.; Gali-Muhtasib, H.; Machaca, K., Copper chelation selectively kills colon cancer cells through redox cycling and generation of reactive oxygen species. *BMC Cancer* **2014,** *14* (1), 527.
101. Steinbrueck, A.; Sedgwick, A. C.; Brewster, J. T.; Yan, K.-C.; Shang, Y.; Knoll, D. M.; Vargas-Zúñiga, G. I.; He, X.-P.; Tian, H.; Sessler, J. L., Transition metal chelators, pro-chelators, and ionophores as small molecule cancer chemotherapeutic agents. *Chem. Soc. Rev.* **2020,** *49* (12), 3726-3747.
102. Richardson, G. S.; Dickersin, G. R.; Atkins, L.; MacLaughlin, D. T.; Raam, S.; Merk, L. P.; Bradley, F. M., KLE: A cell line with defective estrogen receptor derived from undifferentiated endometrial cancer. *Gynecol. Oncol.* **1984,** *17* (2), 213-230.
103. Dahiya, R.; Kwak, K. S.; Byrd, J. C.; Ho, S.; Yoon, W. H.; Kim, Y. S., Mucin synthesis and secretion in various human epithelial cancer cell lines that express the MUC-1 mucin gene. *Cancer Res.* **1993,** *53* (6), 1437-43.
104. Zaman, S.; Yu, X.; Bencivenga, A. F.; Blanden, A. R.; Liu, Y.; Withers, T.; Na, B.; Blayney, A. J.; Gilleran, J.; Boothman, D. A.; Loh, S. N.; Kimball, S. D.; Carpizo, D. R., Combinatorial therapy of zinc metallochaperones with mutant p53 reactivation and diminished copper binding. *Mol. Cancer Ther.* **2019,** *18* (8), 1355-1365.
105. Coe, B. J.; Glenwright, S. J., *Trans*-effects in octahedral transition metal complexes. *Coord. Chem. Rev.* **2000,** *203* (1), 5-80.
106. Jancsó, A.; Gyurcsik, B.; Mesterházy, E.; Berkecz, R., Competition of zinc(II) with cadmium(II) or mercury(II) in binding to a 12-mer peptide. *J. Inorg. Biochem.* **2013,** *126*, 96-103.
107. Sun, Q.; Li, Y.; Shi, H.; Wang, Y.; Zhang, J.; Zhang, Q., Ruthenium complexes as promising candidates against lung cancer. *Molecules* **2021,** *26* (15).
108. Singh Sekhon, B., Metallochaperones - An overview. *Curr. Chem. Biol.* **2010,** *4* (2), 173-186.